SMAI-JCM
SMAI Journal of Computational Mathematics

Analytical approach to Galerkin BEMs on polyhedral surfaces

Norbert G. W. Warncke, Ioana Ciotir, Antoine Tonnoir, Zoé Lambert & Christian Gout

Volume S5 (2019), p. 27-46.
<http://smai-jcm.centre-mersenne.org/item?id=SMAI-JCM_2019__S5__27_0>

Publication membre du
Centre Mersenne pour l'édition scientifique ouverte
http://www.centre-mersenne.org/

Sousmission sur https://smai-jcm.math.cnrs.fr/index.php/SMAI-JCM

SMAI Journal of Computational Mathematics
Vol. S5, 27-46 (2019)

Analytical approach to Galerkin BEMs on polyhedral surfaces

Norbert G. W. Warncke [1]
Ioana Ciotir [2]
Antoine Tonnoir [3]
Zoé Lambert [4]
Christian Gout [5]

[1] Siemens Gamesa Renewable Energy
E-mail address: norbert.warncke@siemensgamesa.com
[2] LMI, Normandie Univ., INSA Rouen, 76000 Rouen, France
E-mail address: ioana.ciotir@insa-rouen.fr
[3] LMI, Normandie Univ., INSA Rouen, 76000 Rouen, France
E-mail address: antoine.tonnoir@insa-rouen.fr
[4] LMI, Normandie Univ., INSA Rouen, 76000 Rouen, France
E-mail address: zoe.lambert@insa-rouen.fr
[5] LMI, Normandie Univ., INSA Rouen, 76000 Rouen, France; and Magique 3D - Advanced 3D Numerical Modeling in Geophysics, Inria Bordeaux - Sud-Ouest [Pau], France
E-mail address: christian.gout@insa-rouen.fr.

Abstract. In this paper, we present a contribution linked to the mini symposium (MS) *Mathematical tools in energy industry* (organised at Arcachon during the 9th International conference Curves and Surfaces). Boundary Element Methods (BEM) have recently had a renewed interest in the field of wind energy as they allow to model more of the unsteady flow phenomena around wind turbine airfoils than Blade Element Momentum theory. Though being computationally more complex, their costs are still significantly lower than CFD methods, placing them in a sweet-spot for the validation of turbine designs under various conditions (yaw, turbulent wind). Based on the results of Lenoir and Salles ([8, 9]), the aim of this work is to find generalised formulas for some integrals involved in Galerkin BEM method for efficient parallelisation and to reduce the computational costs wherever possible.

Keywords. Numerical analysis, approximation, energy, HPC, finite elements method, boundary element methods, Galerkin method, DG method.

1. Introduction

This work is linked to a mini symposium (MS) organised during the 9th international conference Curves and Surfaces (Arcachon, June-July 2018). The MS was oriented toward mathematical modelling and numerical simulations for energy applications in industry, as introduced in *Mathematical tools in energy industry (see* [2, 3, 5]*)*. In this paper, we present a contribution linked to an analytical approach to Galerkin BEMs on polyhedral surfaces.

1.1. General context

Boundary Element Methods have practical applications in Wind Energy for simulating the Aerodynamics of a wind turbine. Due to the high Reynolds number flows, potential flow models are good approximations for attached flows, and the acceptable computational costs of the method allow for full aeroelastic simulations in combination with structural solvers. Nevertheless, there is a continuous demand for optimisation due to the ever-increasing requirements for parameter studies in the design process as well as extensive numerical calculations for the certifications.

This work describes a part of the ongoing optimisation process towards better BEM models at Siemens Gamesa Renewable Energy (see appendix D for a short presentation of the company). In the course of replacing existing BEM models based on the Collocation Point method with the Galerkin method, the problem of the increased computational costs became evident. This is the main motivation of this work.

We want to emphasise that our work is based on the results of Lenoir&Salles [8, 9], who found fully closed-form representations of the 4D Galerkin integrals by means of a reduction approach that can be applied to homogeneous integrants. However, the main obstacle for a fully parallelised numerical implementation of their method is in the necessary treatment of several cases that must be distinguished under different conditions. Our contribution is an attempt to find generalized formulas for some integrals involved in Galerkin BEM method for efficient parallelisation and to reduce the computational costs wherever possible.

1.2. A motivating example for the Galerkin method

Let us briefly recall the main features of BEM methods. Using Green's kernel, the idea is to represent the solution outside a bounded domain $\Omega \subset \mathbb{R}^3$ via an integral formula. Then, the problem rewrites only on the boundary $\partial\Omega$ in order to fulfil the boundary conditions. This leads to solve an integral equation of the form:

$$0 = \Phi(\mathbf{y}) + \int_{\partial\Omega} \left(G(\mathbf{x},\mathbf{y}) \frac{\partial \Phi}{\partial \mathbf{n}}(\mathbf{x}) - \frac{\partial G(\mathbf{x},\mathbf{y})}{\partial \mathbf{n}} \Phi(\mathbf{x}) \right) \mathsf{d}S_{\mathbf{x}} \quad \forall \mathbf{y} \in \partial\Omega \tag{1.1}$$

where Φ represents the unknown solution (velocity potential), G is the fundamental solution of the differential operator, and $\mathbf{n} = \mathbf{n}(\mathbf{x})$ the local unit normal vector at $\mathbf{x} \in \partial\Omega$. The main advantage of the BEM is therefore the reduction of a 3D problem to a 2D one. The trade-off is that the matrices resulting from the discretisation are full (compared to sparse matrices obtained with the Finite Element Method, for instance), and the limitation to potential flows in the simulation of fluid flows.

To discretise the integral equation (1.1), a first and simple idea is to impose the equation pointwise. This is the so-called collocation point method. In this case, only "simple" integral terms must be computed that can be obtained analytically, see for instance Hess&Smith [6, 7]. Yet, this simple approach raises many difficulties: the solution strongly depends on the choice of the collocation points and it is not obvious to ensure convergence even with carefully crafted surface meshes, in particular with complex geometry of wind turbine blade. To illustrate that, Figure 1.1 and 1.2 show the solution obtained with a collocation method (Ardema3D, a potential flow solver developed in-house at Siemens Gamesa Renewable Energy) for solving the Laplace equation around the sphere in two cases. A simple shift of the incident flow may lead to locally strong errors.

A natural idea to improve this situation then is to use a Galerkin method. Instead of (1.1), the idea is to solve the following equation:

$$0 = \int_{\partial\Omega} \Phi(\mathbf{y})\Psi(\mathbf{y})\mathsf{d}S_{\mathbf{y}} + \int_{\partial\Omega} \Psi(\mathbf{y}) \int_{\partial\Omega} \left(G(\mathbf{x},\mathbf{y}) \frac{\partial \Phi}{\partial \mathbf{n}}(\mathbf{x}) - \frac{\partial G(\mathbf{x},\mathbf{y})}{\partial \mathbf{n}} \Phi(\mathbf{x}) \right) \mathsf{d}S_{\mathbf{x}} \mathsf{d}S_{\mathbf{y}} \tag{1.2}$$

where Ψ belongs to a set of test functions. This approach presents many advantages compared to collocation method:

(1) It ensures convergence when improving the discretisation,

(2) It usually has a better accuracy even with lower resolution,

(3) It leads to a symmetric and positive definite system matrix.

However, one pays a "price" in the costs of computing the integral terms. Using a quadrature formula, the Galerkin method turns out to be too costly[12, 1] for being used in time-resolved aeroelastic simulations of wind turbines (the system matrix is computed and inverted each time step). This is

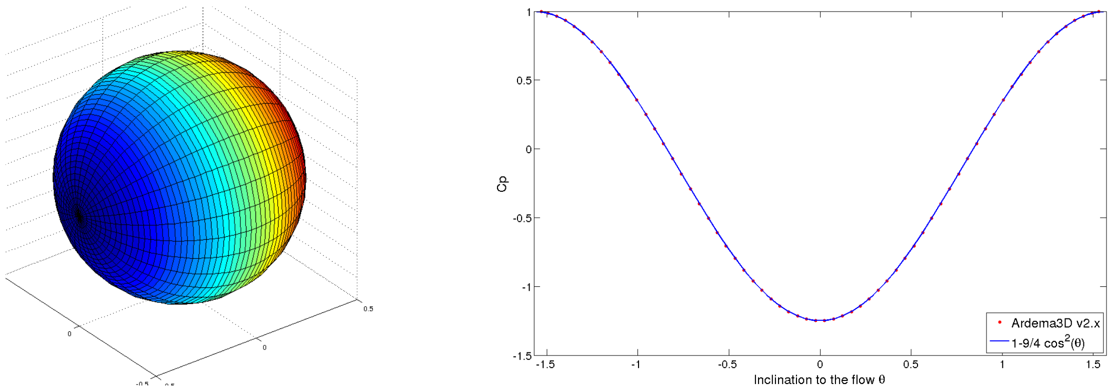

Figure 1.1. Computation of the potential flow around the sphere with perfect incident flow; computed velocity potential over the surface of the sphere (left) and computed surface pressure coefficient $C_p(\theta) = p(\theta)/(\frac{\rho}{2}v_\infty^2)$ in red compared to the analytical solution $C_p(\theta) = 1 - 9/4\cos^2\theta$ in blue (right)

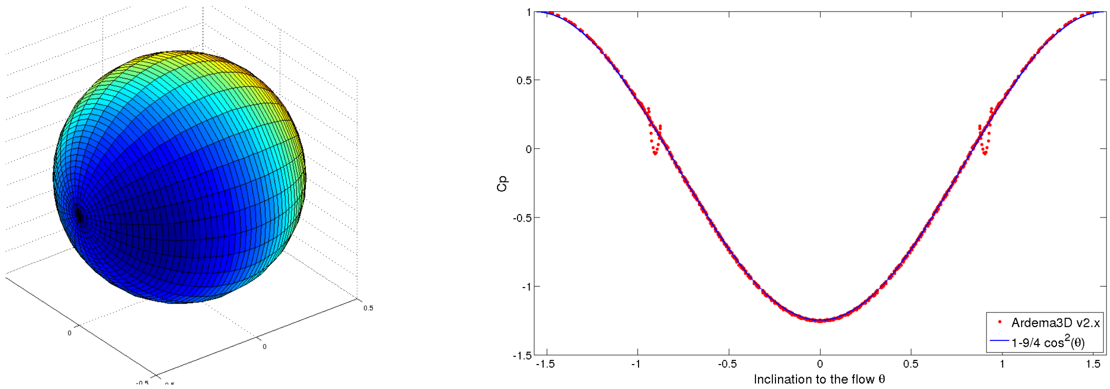

Figure 1.2. Computation of the potential flow around the sphere with oblique incident flow; computed velocity potential over the surface of the sphere (left) and computed surface pressure coefficient $C_p(\theta) = p(\theta)/(\frac{\rho}{2}v_\infty^2)$ in red compared to the analytical solution $C_p(\theta) = 1 - 9/4\cos^2\theta$ in blue (right)

largely due to the singular kernel G that requires many quadrature points for accurate approximations in the near-field.

Recently, closed-form solutions for the computations of the integral terms have been proposed in the work of Lenoir&Salles [8, 9]. The main idea is the decomposition of the 4D kernel integrals into sums of integrals of lower dimension, and to continue this decomposition until only 1D integrals remain that are then solved analytically. The idea of our work is to decompose only up to 2D integrals and to find "elegant" solutions for the arising integrals. The main benefit of this approach is that the computationally expensive handling of different cases (self-influence, co-planar and non-co-planar triangles, and triangles in parallel planes) can be avoided by having general expressions for the remaining 2D integrals. Furthermore, they are also simplified and less costly to compute.

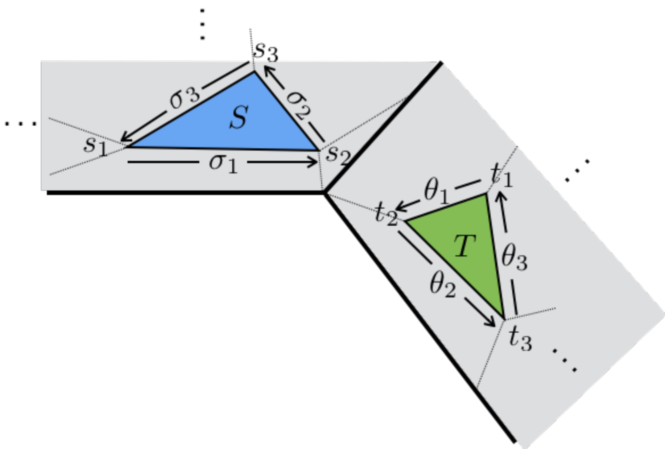

FIGURE 2.1. Schema and notations for two triangular flat patches S and T.

2. Decomposition of the weakly singular kernel

Classically, the three kernel integrals arising in the Galerkin BEM are [12]:

$$\text{weekly singular kernel:} \qquad V = \int_{\mathbf{y}\in T}\int_{\mathbf{x}\in S} G(\mathbf{x},\mathbf{y})\mathrm{d}S\mathrm{d}T \tag{2.1}$$

$$\text{strongly singular kernel:} \qquad K = \int_{\mathbf{y}\in T}\int_{\mathbf{x}\in S} \frac{\partial G(\mathbf{x},\mathbf{y})}{\partial \mathbf{n}_j}\mathrm{d}S\mathrm{d}T \tag{2.2}$$

$$\text{hypersingular kernel:} \qquad W = \int_{\mathbf{y}\in T}\int_{\mathbf{x}\in S} \frac{\partial^2 G(\mathbf{x},\mathbf{y})}{\partial \mathbf{n}_j\partial \mathbf{n}_i}\mathrm{d}S\mathrm{d}T \tag{2.3}$$

where S and T are two flat polygonal surface patches that are typically part of a surface triangulation, see Figure 2.1. In the following we consider the Green's function for the Laplacian in 3D

$$G(\mathbf{x},\mathbf{y}) = \frac{1}{4\pi|\mathbf{x}-\mathbf{y}|}\ . \tag{2.4}$$

Let us introduce some useful notations for the next, summarized in Figure 2.1. The M corner vertices of the polygonal surface patch S are denoted by $\mathbf{s}_i$, and the N corner vertices of T are denoted by $\mathbf{t}_j$. The edges of the polygons are

$$\boldsymbol{\sigma}_i = \mathbf{s}_i + s(\mathbf{s}_{i++} - \mathbf{s}_i), \quad s\in[0,1] \quad \text{and} \quad \boldsymbol{\theta}_j = \mathbf{t}_j + t(\mathbf{t}_{j++} - \mathbf{t}_j), t\in[0,1]$$

each defined from vertex $i = 1,\ldots,M$ to its cyclic successor vertex $i{++} = mod(i,M)+1$, respectively. For a more compact notation, it is convenient to introduce the distance vector

$$\boldsymbol{\Delta}_{j,i} = \mathbf{t}_j - \mathbf{s}_i, \quad \boldsymbol{\Delta}_j = \mathbf{t}_{j++} - \mathbf{t}_j \quad \text{and} \quad \boldsymbol{\Delta}_i = \mathbf{s}_{i++} - \mathbf{s}_i$$

where indices j or $j{++}$ imply an end point of $\boldsymbol{\theta}_j$ and indices i and $i{++}$ end points of $\boldsymbol{\sigma}_i$. We denote also the distance $\Delta_{ij} = |\boldsymbol{\Delta}_{ij}| = |\mathbf{t}_j - \mathbf{s}_i|$. Let us emphasize that when integrating along lines, in some cases the differential element $\mathrm{d}\boldsymbol{\sigma} = (\mathbf{s}_{i++} - \mathbf{s}_i)\mathrm{d}s = \boldsymbol{\Delta}_i\mathrm{d}s$ is vector valued, just as is $\mathrm{d}\boldsymbol{\theta} = (\mathbf{t}_{j++} - \mathbf{t}_j)\mathrm{d}t = \boldsymbol{\Delta}_j\mathrm{d}t$. The scalar differential element is denoted by $\mathrm{d}\sigma = \Delta_i\mathrm{d}s$ and $\mathrm{d}\theta = \Delta_j\mathrm{d}t$. Each edge of a polygonal surface patch has the unit direction vector

$$\hat{\mathbf{s}}_i = (\mathbf{s}_{i++} - \mathbf{s}_i)/|\mathbf{s}_{i++} - \mathbf{s}_i| = \boldsymbol{\Delta}_i/\Delta_i \quad \text{and} \quad \hat{\mathbf{t}}_j = (\mathbf{t}_{j++} - \mathbf{t}_j)/|\mathbf{t}_{j++} - \mathbf{t}_j| = \boldsymbol{\Delta}_j/\Delta_j.$$

Finally, we will denote by

$$\mathbf{n}_S = \frac{\mathbf{\Delta}_i \times \mathbf{\Delta}_{i++}}{|\mathbf{\Delta}_i \times \mathbf{\Delta}_{i++}|} \quad \text{and} \quad \mathbf{n}_T = \frac{\mathbf{\Delta}_j \times \mathbf{\Delta}_{j++}}{|\mathbf{\Delta}_j \times \mathbf{\Delta}_{j++}|}$$

the unit normals to the patches S and T. Let us also notice that in the next, the bilinearform $\langle .,. \rangle$ represents the Euclidean inner product in $\mathbb{R}^3$ and we use the notation $|\mathbf{a}, \mathbf{b}, \mathbf{c}| = \langle \mathbf{a}, \mathbf{b} \times \mathbf{c} \rangle$ for the determinant $\det([\mathbf{a}, \mathbf{b}, \mathbf{c}])$ that typically represents a signed distance (i.e. a projection of a distance vector onto a unit vector perpendicular to one side of the polygonal patch and its normal).

Lenoir&Salles [8, 9] distinguish four different cases: the self-influence (identical patches), co-planar patches, patches in parallel and in secant planes. The first three are special cases of $|\langle \mathbf{n}_S, \mathbf{n}_T \rangle| = 1$ and the last case corresponds to $|\langle \mathbf{n}_S, \mathbf{n}_T \rangle| < 1$. The cases differ in the choices made for the origin that allows the application of the reduction formula while maintaining an homogeneous integrant. Nonetheless, the decompositions into integrals of lower dimension are all similar up to the distance factors that depend on the choice of the origin. The focus of this work is to find solutions for the integrals of dimension 2 (meaning after two steps of reduction) that are not subject to the constraints of the decompositions (meaning $|\langle \mathbf{n}_S, \mathbf{n}_T \rangle| < 1$ or $|\langle \mathbf{n}_S, \mathbf{n}_T \rangle| = 1$). Therefore, just for pedagogical purpose, we will consider the special case of patches in non-parallel planes, i.e. $|\langle \mathbf{n}_S, \mathbf{n}_T \rangle| < 1$, as in Figure 2.1. In that case, both planes cross on a line, where an origin $\mathbf{o} = \mathbf{o}(S, T)$ is chosen. This origin point is defined up to a multiple of $\mathbf{n}_S \times \mathbf{n}_T$, the direction vector of the line defined by the intersection of the two planes.

The first two steps of the decomposition of the 4D integral explained in [8] are:

$$\begin{aligned} V(S,T) &= \int_{\mathbf{y}\in S} \int_{\mathbf{x}\in T} \frac{1}{4\pi|\mathbf{x}-\mathbf{y}|} \mathsf{d}S \mathsf{d}T \\ &= \frac{1}{3}\sum_{i=1}^{M} \underbrace{|\hat{\mathbf{s}}_i, \mathbf{n}_S, \mathbf{o}-\mathbf{s}_i|}_{=d(\mathbf{o},\boldsymbol{\sigma}_i)} U(\boldsymbol{\sigma}_i, T) + \frac{1}{3}\sum_{j=1}^{N} \underbrace{|\hat{\mathbf{t}}_j, \mathbf{n}_T, \mathbf{o}-\mathbf{t}_j|}_{=d(\mathbf{o},\boldsymbol{\theta}_j)} U(\boldsymbol{\theta}_j, S) \end{aligned} \tag{2.5}$$

where $U(\boldsymbol{\sigma}_i, T)$ is a projection of the edge $\boldsymbol{\sigma}_i$ onto the polyhedral patch T and is defined by:

$$U(\boldsymbol{\sigma}_i, T) = \int_{\mathbf{y}\in\boldsymbol{\sigma}_i} \int_{\mathbf{x}\in T} \frac{1}{4\pi|\mathbf{x}-\mathbf{y}|} \mathsf{d}\boldsymbol{\sigma}_i \mathsf{d}T$$

This 3D integral can also be reduced to 2D integrals as follows:

$$U(\boldsymbol{\sigma}_i, T) = \frac{1}{2} \underbrace{|\mathbf{s}_{i++} - \mathbf{o}_{\boldsymbol{\sigma}_i,T}|}_{=d(\mathbf{s}_{i++}, o_{\boldsymbol{\sigma}_i,T})} P(\mathbf{s}_{i++}, T) - \frac{1}{2} \underbrace{|\mathbf{s}_i - o_{\boldsymbol{\sigma}_i,T}|}_{=d(\mathbf{s}_i, o_{\boldsymbol{\sigma}_i,T})} P(\mathbf{s}_i, T) + \frac{1}{2}\sum_{j=1}^{N} \underbrace{|(\mathbf{s}_i - \mathbf{t}_j) \times \hat{\mathbf{t}}_j|}_{=d(\mathbf{s}_i,\boldsymbol{\theta}_j)} Q(\boldsymbol{\sigma}_i, \boldsymbol{\theta}_j) \tag{2.6}$$

where $\mathbf{o}_{\boldsymbol{\sigma}_i,T}$ is the intersection of line $\boldsymbol{\sigma}_i$ with the plane of T. The resulting integrals $P(\mathbf{y}, T)$ and $Q(\boldsymbol{\sigma}_i, \boldsymbol{\theta}_j)$ are 2D integrals that we will study in more details in the next sections. Let us emphasize that one could continue the process of dimension reduction as in the work of Lenoir & Salles [8]. In our case, we will not use this method and we will show how to directly get analytical and efficient (in terms of computational cost) expressions for these integrals.

For the subsequent analysis, an often arising integral is given by the following lemma:

Lemma 2.1. *The solutions of the 1D integral over the weakly singular kernel are*

$$\begin{aligned}
\int_{\mathbf{y}\in\boldsymbol{\sigma}_i} \frac{1}{4\pi|\mathbf{x}-\mathbf{y}|}\mathrm{d}\sigma_i &= -\frac{1}{4\pi}\log\frac{\langle \mathbf{x}-\mathbf{s}_{i++},\hat{\mathbf{s}}_i\rangle + |\mathbf{x}-\mathbf{s}_{i++}|}{\langle \mathbf{x}-\mathbf{s}_i,\hat{\mathbf{s}}_i\rangle + |\mathbf{x}-\mathbf{s}_i|} && \text{(2.7a)}\\
&= \frac{1}{4\pi}\log\frac{|\mathbf{x}-\mathbf{s}_{i++}| - \langle \mathbf{x}-\mathbf{s}_{i++},\hat{\mathbf{s}}_i\rangle}{|\mathbf{x}-\mathbf{s}_i| - \langle \mathbf{x}-\mathbf{s}_i,\hat{\mathbf{s}}_i\rangle} && \text{(2.7b)}\\
&= -\frac{1}{4\pi}\log\frac{|\mathbf{x}-\mathbf{s}_i| + |\mathbf{x}-\mathbf{s}_{i++}| + |\mathbf{s}_{i++}-\mathbf{s}_i|}{|\mathbf{x}-\mathbf{s}_i| + |\mathbf{x}-\mathbf{s}_{i++}| - |\mathbf{s}_{i++}-\mathbf{s}_i|} && \text{(2.7c)}\\
&= -\frac{1}{2\pi}\operatorname{arcoth}\frac{|\mathbf{x}-\mathbf{s}_i| + |\mathbf{x}-\mathbf{s}_{i++}|}{|\mathbf{s}_{i++}-\mathbf{s}_i|} && \text{(2.7d)}\\
&= -\frac{1}{4\pi}\left(\operatorname{arsinh}\frac{\langle \mathbf{x}-\mathbf{s}_{i++},\hat{\mathbf{s}}_i\rangle}{|(\mathbf{x}-\mathbf{s}_{i++})\times\hat{\mathbf{s}}_i|} - \operatorname{arsinh}\frac{\langle \mathbf{x}-\mathbf{s}_i,\hat{\mathbf{s}}_i\rangle}{|(\mathbf{x}-\mathbf{s}_i)\times\hat{\mathbf{s}}_i|}\right) && \text{(2.7e)}
\end{aligned}$$

The proof is only technical and can be found in the appendix.

Let us remark that the different solutions (2.7a) to (2.7e) exist as they all serve different purposes. (2.7a) has a numerical singularity for $\mathbf{x}$ on the extension of the line s_i and $\langle \mathbf{x}-\mathbf{s}_i,\hat{\mathbf{s}}_i\rangle < 0$, the same is valid for (2.7b) in the opposite direction. Therefore, the numerically most robust solution is (2.7c), as it has the singularity only on the line itself. (2.7d) is useful as approximate solution in the far field where it has a series expansion that converges quadratically. As shown in the following, (2.7e) is the most useful solution for further analytical analysis. It is furthermore possible to find other solutions: setting $\tan(z) = \frac{\langle \mathbf{x}-\mathbf{s}_i,\hat{\mathbf{s}}_i\rangle}{|(\mathbf{x}-\mathbf{s}_i)\times\hat{\mathbf{s}}_i|}$ relates (2.7e) to the inverse Gudermannian function $\mathrm{gd}^{-1}(z) = \operatorname{arsinh}(\tan(z))$, which has many other representations [10].

3. Optimal closed-form solution of $P(\mathbf{x}, S)$

The $P(\mathbf{x}, S)$ integral is given by

$$\begin{aligned}
P(\mathbf{x},S) &= \int_{\mathbf{y}\in S}\frac{1}{4\pi|\mathbf{x}-\mathbf{y}|}\mathrm{d}S\\
&= \sum_{i=1}^{N}\frac{|\hat{\mathbf{s}}_i,\mathbf{x}-\mathbf{s}_{i++},\mathbf{n}_S|}{4\pi}\log\frac{|\mathbf{x}-\mathbf{s}_i| + |\mathbf{x}-\mathbf{s}_{i++}| + |\mathbf{s}_{i++}-\mathbf{s}_i|}{|\mathbf{x}-\mathbf{s}_i| + |\mathbf{x}-\mathbf{s}_{i++}| - |\mathbf{s}_{i++}-\mathbf{s}_i|}\\
&+ \frac{|\langle\mathbf{n}_S,\mathbf{x}-\mathbf{s}_1\rangle|}{2\pi}\sum_{i=1}^{N}\Bigg(\arctan\frac{\langle \mathbf{x}-\mathbf{s}_{i++},\hat{\mathbf{s}}_i\rangle - |\langle\mathbf{n}_S,\mathbf{x}-\mathbf{s}_1\rangle| - |\mathbf{x}-\mathbf{s}_{i++}|}{|\mathbf{x}-\mathbf{s}_i,\mathbf{x}-\mathbf{s}_{i++},\mathbf{n}_S|}\\
&\qquad - \arctan\frac{\langle \mathbf{x}-\mathbf{s}_i,\hat{\mathbf{s}}_i\rangle - |\langle\mathbf{n}_S,\mathbf{x}-\mathbf{s}_1\rangle| - |\mathbf{x}-\mathbf{s}_i|}{|\mathbf{x}-\mathbf{s}_i,\mathbf{x}-\mathbf{s}_{i++},\mathbf{n}_S|}\Bigg) \qquad \text{(3.1)}
\end{aligned}$$

It can be interpreted as the potential induced by the polyhedral patch T with a constant unit source strength at the point $\mathbf{x}$. It is essential for analytical Boundary Element Methods based on the Collocation Points, and has as such been studied extensively in the literature. An often cited early solution is [6], a more recent derivation can be found in [4]. They also show that the second sum over the arctan terms is identical to the induced potential of the polyhedral patch with a constant unit dipole strength

$$\frac{\operatorname{sgn}(\langle \mathbf{n}_S, \mathbf{x}-\mathbf{s}_1\rangle)}{2\pi}\sum_{i=1}^{N}\Bigg(\arctan\frac{\langle \mathbf{x}-\mathbf{s}_{i++}, \hat{\mathbf{s}}_i\rangle - |\langle \mathbf{n}_S, \mathbf{x}-\mathbf{s}_1\rangle| - |\mathbf{x}-\mathbf{s}_{i++}|}{|\mathbf{x}-\mathbf{s}_i, \mathbf{x}-\mathbf{s}_{i++}, \mathbf{n}_S|} - \arctan\frac{\langle \mathbf{x}-\mathbf{s}_i, \hat{\mathbf{s}}_i\rangle - |\langle \mathbf{n}_S, \mathbf{x}-\mathbf{s}_1\rangle| - |\mathbf{x}-\mathbf{s}_i|}{|\mathbf{x}-\mathbf{s}_i, \mathbf{x}-\mathbf{s}_{i++}, \mathbf{n}_S|}\Bigg) = \int_{\mathbf{y}\in S}\frac{\langle \mathbf{n}_S, \mathbf{x}-\mathbf{y}\rangle}{4\pi|\mathbf{x}-\mathbf{y}|^3}\mathsf{d}S = \int_{\mathbf{y}\in S}\left\langle \mathbf{n}_S, \nabla\frac{1}{4\pi|\mathbf{x}-\mathbf{y}|}\right\rangle\mathsf{d}S \tag{3.2}$$

Integral (3.2) has the geometric interpretation of the solid angle, i.e. the area that the patch projects on the unit sphere centered at $\mathbf{x}$. In particular, Van Oosterom&Strackee[13] found a very efficient formula for the solid angle of a *planar triangle*

$$\Omega_\Delta = \int_{\mathbf{y}\in S_\Delta}\left\langle \mathbf{n}_{S_\Delta}, \nabla\frac{1}{|\mathbf{x}-\mathbf{y}|}\right\rangle\mathsf{d}S_\Delta = 2\arctan\frac{\left|\frac{\mathbf{x}-\mathbf{s}_1}{|\mathbf{x}-\mathbf{s}_1|}, \frac{\mathbf{x}-\mathbf{s}_2}{|\mathbf{x}-\mathbf{s}_2|}, \frac{\mathbf{x}-\mathbf{s}_3}{|\mathbf{x}-\mathbf{s}_3|}\right|}{1+\frac{\langle \mathbf{x}-\mathbf{s}_1, \mathbf{x}-\mathbf{s}_2\rangle}{|\mathbf{x}-\mathbf{s}_1||\mathbf{x}-\mathbf{s}_2|}+\frac{\langle \mathbf{x}-\mathbf{s}_2, \mathbf{x}-\mathbf{s}_3\rangle}{|\mathbf{x}-\mathbf{s}_2||\mathbf{x}-\mathbf{s}_3|}+\frac{\langle \mathbf{x}-\mathbf{s}_3, \mathbf{x}-\mathbf{s}_1\rangle}{|\mathbf{x}-\mathbf{s}_3||\mathbf{x}-\mathbf{s}_1|}} \tag{3.3}$$

where S_Δ denotes a triangle patch. Equation (3.3) is computationally more efficient and also numerically more robust than the sum of differences of the arctan terms, even if the latter are combined via summation identities. Let us emphasize that for a *quadrilateral patch*, it is also advisable to decompose it into two sub-triangles and apply (3.3). The direct summation with formula (3.2) is only asymptotically more efficient for polyhedral patches with many sides.

For a *triangular surface* patch, the optimal solution for $P(\mathbf{x}, S)$ is then given combining (3.1) and (3.3) by

$$P(\mathbf{x}, S) = \sum_{i=1}^{3}\frac{|\hat{\mathbf{s}}_i, \mathbf{x}-\mathbf{s}_{i++}, \mathbf{n}_S|}{4\pi}\log\frac{|\mathbf{x}-\mathbf{s}_i|+|\mathbf{x}-\mathbf{s}_{i++}|+|\mathbf{s}_{i++}-\mathbf{s}_i|}{|\mathbf{x}-\mathbf{s}_i|+|\mathbf{x}-\mathbf{s}_{i++}|-|\mathbf{s}_{i++}-\mathbf{s}_i|} + \frac{\langle \mathbf{n}_S, \mathbf{x}-\mathbf{s}_1\rangle}{2\pi}\arctan\frac{\left|\frac{\mathbf{x}-\mathbf{s}_1}{|\mathbf{x}-\mathbf{s}_1|}, \frac{\mathbf{x}-\mathbf{s}_2}{|\mathbf{x}-\mathbf{s}_2|}, \frac{\mathbf{x}-\mathbf{s}_3}{|\mathbf{x}-\mathbf{s}_3|}\right|}{1+\frac{\langle \mathbf{x}-\mathbf{s}_1, \mathbf{x}-\mathbf{s}_2\rangle}{|\mathbf{x}-\mathbf{s}_1||\mathbf{x}-\mathbf{s}_2|}+\frac{\langle \mathbf{x}-\mathbf{s}_2, \mathbf{x}-\mathbf{s}_3\rangle}{|\mathbf{x}-\mathbf{s}_2||\mathbf{x}-\mathbf{s}_3|}+\frac{\langle \mathbf{x}-\mathbf{s}_3, \mathbf{x}-\mathbf{s}_1\rangle}{|\mathbf{x}-\mathbf{s}_3||\mathbf{x}-\mathbf{s}_1|}} \tag{3.4}$$

Remark 3.1. Let us remark that from the perspective of decomposing integrals over homogeneous kernels, (3.1) together with (3.2) has the structure

$$P(\mathbf{x}, S) = \sum_{i=1}^{N}|\hat{\mathbf{s}}_i, \mathbf{x}-\mathbf{s}_{i++}, \mathbf{n}_S|\int_{\mathbf{y}\in\boldsymbol{\sigma}_i}\frac{1}{4\pi|\mathbf{x}-\mathbf{y}|}\mathsf{d}\sigma_i + \langle \mathbf{n}_S, \mathbf{x}-\mathbf{s}_1\rangle\int_{\mathbf{y}\in S}\left\langle \mathbf{n}_S, \nabla\frac{1}{4\pi|\mathbf{x}-\mathbf{y}|}\right\rangle\mathsf{d}S \tag{3.5}$$

The origin $\mathbf{o} = (\mathbb{1} - \mathbf{n}_S\mathbf{n}_S^T)(\mathbf{x}-\mathbf{s}_i) + \mathbf{s}_i$ for this decomposition is the point on the plane defined by S that is closest to $\mathbf{x}$. This choice was made implicitly by [4] and [6] for finding a coordinate system that allows an analytical solution of the integral. The decomposition is not obvious, as the second term still contains a 2D integral and therefore does not simplify the problem much. This term is still the product of a projected length times an integral, only that in this case the replacing integral can be solved efficiently due to its geometric interpretation as the solid angle. This naturally raises the question if the decomposition steps (2.5) and (2.6) are optimal in the sense of yielding the most simple expressions. There is unfortunately no known answer to this question yet.

4. General closed-form solution of $Q(\boldsymbol{\sigma}_i, \boldsymbol{\theta}_j)$

The second term of the decomposition of (2.6) leads to a double line integral over the weakly singular kernel

$$Q(\boldsymbol{\sigma}_i, \boldsymbol{\theta}_j) = \int_{\mathbf{x}\in\boldsymbol{\theta}_j} \int_{\mathbf{y}\in\boldsymbol{\sigma}_i} \frac{\mathsf{d}\sigma_i, \mathsf{d}\theta_j}{4\pi|\mathbf{x}-\mathbf{y}|} \ . \tag{4.1}$$

Remark 4.1. Let us remark that (4.1) shows similarities with equation (5.2) presented later; the hypersingular kernel for the Green's function (2.4) of two polyhedral patches S and T is in fact the summation of the contribution Q of all pairs of sides

$$W = \sum_i \sum_j \langle \hat{\mathbf{s}}_i, \hat{\mathbf{t}}_j \rangle \ Q(\boldsymbol{\sigma}_i, \boldsymbol{\theta}_j) \ . \tag{4.2}$$

To solve (4.1), the inner integral can be written down directly with the help of Lemma 2.1. We choose the solution via the arsinh terms, all other solutions result in very complex integrants.

$$\begin{aligned} Q(\boldsymbol{\sigma}_i, \boldsymbol{\theta}_j) &= -\frac{1}{4\pi} \int_{\mathbf{x}\in\boldsymbol{\theta}_j} \left(\operatorname{arsinh} \frac{\langle \mathbf{x}-\mathbf{s}_{i++}, \hat{\mathbf{s}}_i\rangle}{|(\mathbf{x}-\mathbf{s}_{i++})\times\hat{\mathbf{s}}_i|} - \operatorname{arsinh} \frac{\langle \mathbf{x}-\mathbf{s}_{i}, \hat{\mathbf{s}}_i\rangle}{|(\mathbf{x}-\mathbf{s}_{i})\times\hat{\mathbf{s}}_i|} \right) \mathsf{d}\theta_j \\ &= \frac{1}{4\pi} \underbrace{\int_{\mathbf{x}\in\boldsymbol{\theta}_j} \operatorname{arsinh} \frac{\langle \mathbf{x}-\mathbf{s}_{i}, \hat{\mathbf{s}}_i\rangle}{|(\mathbf{x}-\mathbf{s}_{i})\times\hat{\mathbf{s}}_i|} \mathsf{d}\theta_j}_{=Q_i} - \frac{1}{4\pi} \underbrace{\int_{\mathbf{x}\in\boldsymbol{\theta}_j} \operatorname{arsinh} \frac{\langle \mathbf{x}-\mathbf{s}_{i++}, \hat{\mathbf{s}}_i\rangle}{|(\mathbf{x}-\mathbf{s}_{i++})\times\hat{\mathbf{s}}_i|} \mathsf{d}\theta_j}_{=Q_{i++}} \end{aligned} \tag{4.3}$$

Q_i and Q_{i++} represent the integrals over one of the arsinh terms. Their solution only differs by the choice of $\mathbf{s}_i$ or $\mathbf{s}_{i++}$, which are both constant parameters for the integrals. In the following, the solution of Q_i will be calculated explicitly, and the analog solution Q_{i++} can be obtained by replacing $\mathbf{s}_i$ with $\mathbf{s}_{i++}$.

Before going further in the computations of the Q integral, it is helpful to introduce the two following lemmas:

Lemma 4.2.

$$\begin{aligned} \int \operatorname{arsinh} \frac{a+bz}{\sqrt{z^2+c^2}} \mathsf{d}z = z \operatorname{arsinh} \frac{a+bz}{\sqrt{z^2+c^2}} - c \arctan \frac{az-bc^2}{c\sqrt{(a+bz)^2+z^2+c^2}} \\ + \frac{a}{\sqrt{b^2+1}} \log(\sqrt{b^2+1}\sqrt{(a+bz)^2+z^2+c^2} + b(a+bz)+z) + \text{const.} \end{aligned} \tag{4.4}$$

Lemma 4.3.

$$\int \operatorname{arsinh}(a+bz)\mathsf{d}z = \frac{(a+bz)\operatorname{arsinh}(a+bz) - \sqrt{(a+bz)^2+1}}{b} + \text{const.} \tag{4.5}$$

The proofs are again mainly technical and can be found in the appendix.

4.1. General skewed lines

Assuming that $\boldsymbol{\sigma}_i$ and $\boldsymbol{\theta}_j$ are not parallel, it follows that $\hat{\mathbf{t}}_j \times \hat{\mathbf{s}}_i \neq 0$ where we recall that $\boldsymbol{\Delta}_j = \hat{\mathbf{t}}_j|\boldsymbol{\Delta}_j|$ and $\boldsymbol{\Delta}_i = \hat{\mathbf{s}}_i|\boldsymbol{\Delta}_i|$. Considering the Q_i integral term and recalling that $\boldsymbol{\theta}_j = \mathbf{t}_j + t(\mathbf{t}_{j++} - \mathbf{t}_j) = \mathbf{t}_j + t\boldsymbol{\Delta}_j$,

$t \in [0,1]$, with $\mathsf{d}\theta_j = \Delta_j \mathsf{d}t$, and using (4.4) leads after substitution to:

$$
\begin{aligned}
Q_i &= \int_{\mathbf{x}\in\boldsymbol{\theta}_j} \operatorname{arsinh} \frac{\langle \mathbf{x}-\mathbf{s}_i, \hat{\mathbf{s}}_i\rangle}{|(\mathbf{x}-\mathbf{s}_i)\times\hat{\mathbf{s}}_i|}\mathsf{d}\theta_j = \Delta_j \int_0^1 \operatorname{arsinh} \frac{\langle \boldsymbol{\Delta}_{j,i}, \hat{\mathbf{s}}_i\rangle + t\langle \boldsymbol{\Delta}_j, \hat{\mathbf{s}}_i\rangle}{\sqrt{(\boldsymbol{\Delta}_{j,i}\times\hat{\mathbf{s}}_i + t\boldsymbol{\Delta}_j\times\hat{\mathbf{s}}_i)^2}}\mathsf{d}t \\
&= \Delta_j \int_0^1 \operatorname{arsinh} \frac{\langle \boldsymbol{\Delta}_{j,i}, \hat{\mathbf{s}}_i\rangle + t\langle \boldsymbol{\Delta}_j, \hat{\mathbf{s}}_i\rangle}{\sqrt{(\boldsymbol{\Delta}_{j,i}\times\hat{\mathbf{s}}_i)^2 + 2t\langle \boldsymbol{\Delta}_{j,i}\times\hat{\mathbf{s}}_i, \boldsymbol{\Delta}_j\times\hat{\mathbf{s}}_i\rangle + t^2(\boldsymbol{\Delta}_j\times\hat{\mathbf{s}}_i)^2}}\mathsf{d}t \\
&= \Delta_j \int_0^1 \operatorname{arsinh} \frac{\langle \boldsymbol{\Delta}_{j,i}, \hat{\mathbf{s}}_i\rangle + t\langle \boldsymbol{\Delta}_j, \hat{\mathbf{s}}_i\rangle}{\sqrt{\underbrace{|\boldsymbol{\Delta}_{j,i}\times\hat{\mathbf{s}}_i|^2 - \frac{\langle \boldsymbol{\Delta}_{j,i}\times\hat{\mathbf{s}}_i, \hat{\mathbf{t}}_j\times\hat{\mathbf{s}}_i\rangle^2}{|\hat{\mathbf{t}}_j\times\hat{\mathbf{s}}_i|^2}}_{=c_i^2} + \underbrace{\left(\frac{\langle \boldsymbol{\Delta}_{j,i}\times\hat{\mathbf{s}}_i, \hat{\mathbf{t}}_j\times\hat{\mathbf{s}}_i\rangle}{|\hat{\mathbf{t}}_j\times\hat{\mathbf{s}}_i|} + t|\boldsymbol{\Delta}_j\times\hat{\mathbf{s}}_i|\right)^2}_{=z_i^2}}}\mathsf{d}t
\end{aligned} \tag{4.6}
$$

Let us note that the index i above is introduce on c_i and z_i because we study Q_i. Substituting $z_i = \frac{\langle \boldsymbol{\Delta}_{j,i}\times\hat{\mathbf{s}}_i, \hat{\mathbf{t}}_j\times\hat{\mathbf{s}}_i\rangle}{|\hat{\mathbf{t}}_j\times\hat{\mathbf{s}}_i|} + t|\boldsymbol{\Delta}_j\times\hat{\mathbf{s}}_i|$ with $\mathsf{d}z_i = |\boldsymbol{\Delta}_j\times\hat{\mathbf{s}}_i|\mathsf{d}t$ and taking a_i and b_i such that

$$
a_i + b_i z_i = \langle \boldsymbol{\Delta}_{j,i}, \hat{\mathbf{s}}_i\rangle + t\langle \boldsymbol{\Delta}_j, \hat{\mathbf{s}}_i\rangle \quad\Leftrightarrow\quad b_i = \frac{\langle \boldsymbol{\Delta}_j, \hat{\mathbf{s}}_i\rangle}{|\boldsymbol{\Delta}_j\times\hat{\mathbf{s}}_i|} \text{ and } a_i = \langle \boldsymbol{\Delta}_{j,i}, \hat{\mathbf{s}}_i\rangle - b_i\frac{\langle \boldsymbol{\Delta}_{j,i}\times\hat{\mathbf{s}}_i, \hat{\mathbf{t}}_j\times\hat{\mathbf{s}}_i\rangle}{|\hat{\mathbf{t}}_j\times\hat{\mathbf{s}}_i|} \tag{4.7}
$$

then leads by Lemma 4.2 to

$$
\begin{aligned}
Q_i &= \frac{\Delta_j}{|\boldsymbol{\Delta}_j\times\hat{\mathbf{s}}_i|}\int_{z_i(0)}^{z_i(1)} \operatorname{arsinh}\frac{a_i+b_iz_i}{\sqrt{c_i^2+z_i^2}}\mathsf{d}z_i \\
&= \frac{1}{|\hat{\mathbf{t}}_j\times\hat{\mathbf{s}}_i|}\Bigg[z_i \operatorname{arsinh}\frac{a_i+b_iz_i}{\sqrt{z_i^2+c_i^2}} - c_i \arctan\frac{a_iz_i - b_ic_i^2}{c_i\sqrt{(a_i+b_iz_i)^2+z_i^2+c_i^2}} \\
&\qquad + \frac{a_i}{\sqrt{b_i^2+1}}\log\left(\sqrt{b_i^2+1}\sqrt{(a_i+b_iz_i)^2+z_i^2+c_i^2} + b_i(a_i+b_iz_i)+z_i\right)\Bigg]_{z_i(0)}^{z_i(1)}
\end{aligned} \tag{4.8}
$$

In the above formula, the coefficients a_i, b_i, c_i, $z_i(0)$ and $z_i(1)$ can be simplified as follows:

$$
a_i = \frac{\langle \boldsymbol{\Delta}_{j,i}\times\hat{\mathbf{t}}_j, \hat{\mathbf{s}}_i\times\hat{\mathbf{t}}_j\rangle}{|\hat{\mathbf{t}}_j\times\hat{\mathbf{s}}_i|^2} \qquad b_i = \frac{\langle \hat{\mathbf{t}}_j, \hat{\mathbf{s}}_i\rangle}{|\hat{\mathbf{t}}_j\times\hat{\mathbf{s}}_i|} \qquad c_i = \frac{|\hat{\mathbf{s}}_i, \boldsymbol{\Delta}_{j,i}, \hat{\mathbf{t}}_j|}{|\hat{\mathbf{t}}_j\times\hat{\mathbf{s}}_i|}
$$

$$
z_i(0) = \frac{\langle \boldsymbol{\Delta}_{j,i}\times\hat{\mathbf{s}}_i, \hat{\mathbf{t}}_j\times\hat{\mathbf{s}}_i\rangle}{|\hat{\mathbf{t}}_j\times\hat{\mathbf{s}}_i|} \qquad z_i(1) = \frac{\langle \boldsymbol{\Delta}_{j++,i}\times\hat{\mathbf{s}}_i, \hat{\mathbf{t}}_j\times\hat{\mathbf{s}}_i\rangle}{|\hat{\mathbf{t}}_j\times\hat{\mathbf{s}}_i|}
$$

Let us remark that with the above expression of parameter c_i, we can see that c_i can be interpreted as the minimal distance between the (infinitely extended) lines $\boldsymbol{\sigma}_i$ and $\boldsymbol{\theta}_j$. In particular if $c_i = 0$, the problem becomes essentially two-dimensional and the arctan term drops out.

Let us also emphasize that for the computation of Q_{i++} in (4.3), we get a similar result but with the following parameters:

$$
a_{i++} = \frac{\langle \boldsymbol{\Delta}_{j,i++}\times\hat{\mathbf{t}}_j, \hat{\mathbf{s}}_i\times\hat{\mathbf{t}}_j\rangle}{|\hat{\mathbf{t}}_j\times\hat{\mathbf{s}}_i|^2} \qquad b_{i++} = \frac{\langle \hat{\mathbf{t}}_j, \hat{\mathbf{s}}_i\rangle}{|\hat{\mathbf{t}}_j\times\hat{\mathbf{s}}_i|} \qquad c_{i++} = \frac{|\hat{\mathbf{s}}_i, \boldsymbol{\Delta}_{j,i++}, \hat{\mathbf{t}}_j|}{|\hat{\mathbf{t}}_j\times\hat{\mathbf{s}}_i|}
$$

$$
z_{i++}(0) = \frac{\langle \boldsymbol{\Delta}_{j,i++}\times\hat{\mathbf{s}}_i, \hat{\mathbf{t}}_j\times\hat{\mathbf{s}}_i\rangle}{|\hat{\mathbf{t}}_j\times\hat{\mathbf{s}}_i|} \qquad z_{i++}(1) = \frac{\langle \boldsymbol{\Delta}_{j++,i++}\times\hat{\mathbf{s}}_i, \hat{\mathbf{t}}_j\times\hat{\mathbf{s}}_i\rangle}{|\hat{\mathbf{t}}_j\times\hat{\mathbf{s}}_i|}
$$

We can notice that $b_{i++} = b_i$ so we will note in the next simply $b_{i++} = b_i = b$. Moreover, remarking that

$$\mathbf{\Delta}_{k,i++} \times \hat{\mathbf{s}}_i = (\mathbf{t}_k - \mathbf{s}_{i++}) \times \hat{\mathbf{s}}_i = (\mathbf{t}_k - \mathbf{s}_i) \times \hat{\mathbf{s}}_i = \mathbf{\Delta}_{k,i} \times \hat{\mathbf{s}}_i, \quad k = \{j, j++\} \tag{4.9}$$

we can easily check that $c_{i++} = c_i$ so that we will note in the next $c_{i++} = c_i = c$. With the same argument, $z_i(0) = z_{i++}(0) = z(0)$ and $z_i(1) = z_{i++}(1) = z(1)$, allowing to drop the index.

Some more simplifications can be obtained by re-substituting the constant parameters. Indeed, using (4.7), we can see that:

$$a_i + bz(0) = \langle \mathbf{\Delta}_{j,i}, \hat{\mathbf{s}}_i \rangle \quad \text{and} \quad a_i + bz(1) = \langle \mathbf{\Delta}_{j,i}, \hat{\mathbf{s}}_i \rangle + \langle \mathbf{\Delta}_j, \hat{\mathbf{s}}_i \rangle = \langle \mathbf{\Delta}_{j++,i}, \hat{\mathbf{s}}_i \rangle$$

and by definition of z^2 and c^2, using the first line of (4.6), we have

$$z^2(0) + c^2 = |\mathbf{\Delta}_{j,i} \times \hat{\mathbf{s}}_i|^2 \quad \text{and} \quad z^2(1) + c^2 = |\mathbf{\Delta}_{j++,i} \times \hat{\mathbf{s}}_i|^2$$

so that the arsinh term of Q_i becomes

$$\left[z \operatorname{arsinh}\left(\frac{a_i + bz}{\sqrt{z^2 + c^2}} \right) \right]_{z(0)}^{z(1)} = \frac{\langle \mathbf{\Delta}_{j++,i} \times \hat{\mathbf{s}}_i, \hat{\mathbf{t}}_j \times \hat{\mathbf{s}}_i \rangle}{|\hat{\mathbf{t}}_j \times \hat{\mathbf{s}}_i|} \operatorname{arsinh} \frac{\langle \mathbf{\Delta}_{j++,i}, \hat{\mathbf{s}}_i \rangle}{|\mathbf{\Delta}_{j++,i} \times \hat{\mathbf{s}}_i|} - \frac{\langle \mathbf{\Delta}_{j,i} \times \hat{\mathbf{s}}_i, \hat{\mathbf{t}}_j \times \hat{\mathbf{s}}_i \rangle}{|\hat{\mathbf{t}}_j \times \hat{\mathbf{s}}_i|} \operatorname{arsinh} \frac{\langle \mathbf{\Delta}_{j,i}, \hat{\mathbf{s}}_i \rangle}{|\mathbf{\Delta}_{j,i} \times \hat{\mathbf{s}}_i|}$$

Likewise, for Q_{i++} we get with the arsinh term

$$\left[z \operatorname{arsinh}\left(\frac{a_{i++} + bz}{\sqrt{z^2 + c^2}} \right) \right]_{z(0)}^{z(1)} = \frac{\langle \mathbf{\Delta}_{j++,i++} \times \hat{\mathbf{s}}_i, \hat{\mathbf{t}}_j \times \hat{\mathbf{s}}_i \rangle}{|\hat{\mathbf{t}}_j \times \hat{\mathbf{s}}_i|} \operatorname{arsinh} \frac{\langle \mathbf{\Delta}_{j++,i++}, \hat{\mathbf{s}}_i \rangle}{|\mathbf{\Delta}_{j++,i++} \times \hat{\mathbf{s}}_i|} - \frac{\langle \mathbf{\Delta}_{j,i++} \times \hat{\mathbf{s}}_i, \hat{\mathbf{t}}_j \times \hat{\mathbf{s}}_i \rangle}{|\hat{\mathbf{t}}_j \times \hat{\mathbf{s}}_i|} \operatorname{arsinh} \frac{\langle \mathbf{\Delta}_{j,i++}, \hat{\mathbf{s}}_i \rangle}{|\mathbf{\Delta}_{j,i++} \times \hat{\mathbf{s}}_i|}$$

It follows from (4.9) that two arsinh terms can be combined to

$$\begin{aligned}
&\left[z \operatorname{arsinh}\left(\frac{a_{i++} + bz}{\sqrt{z^2 + c^2}} \right) \right]_{z(0)}^{z(1)} - \left[z \operatorname{arsinh}\left(\frac{a_i + bz}{\sqrt{z^2 + c^2}} \right) \right]_{z(0)}^{z(1)} \\
&= \frac{\langle \mathbf{\Delta}_{j++,i} \times \hat{\mathbf{s}}_i, \hat{\mathbf{t}}_j \times \hat{\mathbf{s}}_i \rangle}{|\hat{\mathbf{t}}_j \times \hat{\mathbf{s}}_i|} \left(\operatorname{arsinh} \frac{\langle \mathbf{\Delta}_{j++,i++}, \hat{\mathbf{s}}_i \rangle}{|\mathbf{\Delta}_{j++,i++} \times \hat{\mathbf{s}}_i|} - \operatorname{arsinh} \frac{\langle \mathbf{\Delta}_{j++,i}, \hat{\mathbf{s}}_i \rangle}{|\mathbf{\Delta}_{j++,i} \times \hat{\mathbf{s}}_i|} \right) \\
&\quad - \frac{\langle \mathbf{\Delta}_{j,i++} \times \hat{\mathbf{s}}_i, \hat{\mathbf{t}}_j \times \hat{\mathbf{s}}_i \rangle}{|\hat{\mathbf{t}}_j \times \hat{\mathbf{s}}_i|} \left(\operatorname{arsinh} \frac{\langle \mathbf{\Delta}_{j,i++}, \hat{\mathbf{s}}_i \rangle}{|\mathbf{\Delta}_{j,i++} \times \hat{\mathbf{s}}_i|} - \operatorname{arsinh} \frac{\langle \mathbf{\Delta}_{j,i}, \hat{\mathbf{s}}_i \rangle}{|\mathbf{\Delta}_{j,i} \times \hat{\mathbf{s}}_i|} \right) \\
&= \frac{\langle \mathbf{\Delta}_{j++,i} \times \hat{\mathbf{s}}_i, \hat{\mathbf{t}}_j \times \hat{\mathbf{s}}_i \rangle}{|\hat{\mathbf{t}}_j \times \hat{\mathbf{s}}_i|} \log \frac{\Delta_{j++,i} + \Delta_{j++,i++} + \Delta_i}{\Delta_{j++,i} + \Delta_{j++,i++} - \Delta_i} - \frac{\langle \mathbf{\Delta}_{j,i++} \times \hat{\mathbf{s}}_i, \hat{\mathbf{t}}_j \times \hat{\mathbf{s}}_i \rangle}{|\hat{\mathbf{t}}_j \times \hat{\mathbf{s}}_i|} \log \frac{\Delta_{j,i} + \Delta_{j,i++} + \Delta_i}{\Delta_{j,i} + \Delta_{j,i++} - \Delta_i}
\end{aligned}$$

The replacement of the arsinh terms with the numerically more stable log terms is again a consequence of the equivalence of (2.7c) and (2.7e).

For dealing with the log terms in the expression (4.8) of Q_i, it is helpful to note these identities:

$$\sqrt{(a_i + bz(0))^2 + z(0)^2 + c^2} = \Delta_{j,i} \qquad \sqrt{(a_{i++} + bz(0))^2 + z(0)^2 + c^2} = \Delta_{j,i++}$$

$$\sqrt{(a_i + bz(1))^2 + z(1)^2 + c^2} = \Delta_{j++,i} \qquad \sqrt{(a_{i++} + bz(1))^2 + z(1)^2 + c^2} = \Delta_{j++,i++}$$

These identities can be obtained using the classical result $|\mathbf{u}|^2|\mathbf{v}|^2 = \langle \mathbf{u}, \mathbf{v} \rangle^2 + |\mathbf{u} \times \mathbf{v}|^2$ for any vectors $\mathbf{u}$ and $\mathbf{v}$. Another useful identities are:

$$b(a_i + bz(0)) + z(0) = \frac{\langle \hat{\mathbf{t}}_j, \mathbf{\Delta}_{j,i} \rangle}{|\hat{\mathbf{t}}_j \times \hat{\mathbf{s}}_i|} \qquad \text{and} \qquad \sqrt{b^2 + 1} = \frac{1}{|\hat{\mathbf{t}}_j \times \hat{\mathbf{s}}_i|}.$$

Thanks to these results, the log terms in (4.8) considerably simplify:

$$\left[\frac{a_i}{\sqrt{b^2+1}}\log\left(\sqrt{(a_i+bz)^2+z^2+c^2}+\frac{b(a_i+bz)+z}{\sqrt{b^2+1}}\right)\right]_{z(0)}^{z(1)} \\ = -\frac{\langle \mathbf{\Delta}_{j,i}\times\hat{\mathbf{t}}_j, \hat{\mathbf{s}}_i\times\hat{\mathbf{t}}_j\rangle}{|\hat{\mathbf{t}}_j\times\hat{\mathbf{s}}_i|}\log\frac{\Delta_{j,i}+\Delta_{j++,i}+\Delta_j}{\Delta_{j,i}+\Delta_{j++,i}-\Delta_j}$$

and we similarly get for the log term in Q_{i++}:

$$\left[\frac{a_{i++}}{\sqrt{b^2+1}}\log\left(\sqrt{(a_{i++}+bz)^2+z^2+c^2}+\frac{b(a_{i++}+bz)+z}{\sqrt{b^2+1}}\right)\right]_{z(0)}^{z(1)} \\ = -\frac{\langle \mathbf{\Delta}_{j,i++}\times\hat{\mathbf{t}}_j, \hat{\mathbf{s}}_i\times\hat{\mathbf{t}}_j\rangle}{|\hat{\mathbf{t}}_j\times\hat{\mathbf{s}}_i|}\log\frac{\Delta_{j,i++}+\Delta_{j++,i++}+\Delta_j}{\Delta_{j,i++}+\Delta_{j++,i++}-\Delta_j}$$

Here the equivalence between (2.7c) and (2.7b) was used to obtain a numerically robust representation. Geometrically, these terms are the exact complement of what was obtained from the arsinh terms: the influence from one line onto the end vertices of the other, only with $\boldsymbol{\theta}_j$ replacing $\boldsymbol{\sigma}_i$.

The remaining arctan term of Q_i is more difficult to simplify significantly. Splitting each argument into a numerator N_i and a denominator D_i gives

$$\frac{(a_i z(0)-bc^2)}{c\sqrt{(a_i+b_i z(0))^2+z(0)^2+c^2}} = \frac{\langle \mathbf{\Delta}_{j,i}\times\hat{\mathbf{t}}_j, \hat{\mathbf{s}}_i\times\hat{\mathbf{t}}_j\rangle\langle \mathbf{\Delta}_{j,i}\times\hat{\mathbf{s}}_i, \hat{\mathbf{t}}_j\times\hat{\mathbf{s}}_i\rangle - \langle\hat{\mathbf{t}}_j,\hat{\mathbf{s}}_i\rangle|\hat{\mathbf{s}}_i,\mathbf{\Delta}_{j,i},\hat{\mathbf{t}}_j|^2}{|\hat{\mathbf{s}}_i,\mathbf{\Delta}_{j,i},\hat{\mathbf{t}}_j||\hat{\mathbf{t}}_j\times\hat{\mathbf{s}}_i|^2\Delta_{j,i}} = \frac{N_{i,j}}{D_{i,j}}$$

with

$$\begin{aligned} N_{i,j} &= \langle \mathbf{\Delta}_{j,i}\times\hat{\mathbf{t}}_j, \hat{\mathbf{s}}_i\times\hat{\mathbf{t}}_j\rangle\langle \mathbf{\Delta}_{j,i}\times\hat{\mathbf{s}}_i, \hat{\mathbf{t}}_j\times\hat{\mathbf{s}}_i\rangle - \langle\hat{\mathbf{t}}_j,\hat{\mathbf{s}}_i\rangle|\hat{\mathbf{s}}_i,\mathbf{\Delta}_{j,i},\hat{\mathbf{t}}_j|^2 \\ D_{i,j} &= |\hat{\mathbf{s}}_i,\mathbf{\Delta}_{j,i},\hat{\mathbf{t}}_j||\hat{\mathbf{t}}_j\times\hat{\mathbf{s}}_i|^2\Delta_{j,i} \end{aligned}$$

All other numerators and denominators are obtained by replacing the respective indices. Combining all arctan terms of both integrals then results in

$$c\left[\arctan\frac{a_i z-bc^2}{c\sqrt{(a_i+bz)^2+z^2+c^2}}\right]_{z(0)}^{z(1)} - c\left[\arctan\frac{a_{i++}z-bc^2}{c\sqrt{(a_{i++}+bz)^2+z^2+c^2}}\right]_{z(0)}^{z(1)} \\ = \frac{|\hat{\mathbf{s}}_i,\mathbf{\Delta}_{j,i},\hat{\mathbf{t}}_j|}{|\hat{\mathbf{t}}_j\times\hat{\mathbf{s}}_i|}\left(\arctan\frac{N_{i,j++}}{D_{i,j++}}-\arctan\frac{N_{i,j}}{D_{i,j}}-\arctan\frac{N_{i++,j++}}{D_{i++,j++}}+\arctan\frac{N_{i++,j}}{D_{i++,j}}\right)$$

It is in general advisable to further combine all four terms by using a summation identity, which requires only one evaluation of the `atan2()` function.

Combining all terms gives the solution

$$
\begin{aligned}
Q(\boldsymbol{\sigma}_i, \boldsymbol{\theta}_j) &= \int_{\mathbf{y}\in\boldsymbol{\sigma}_i} \int_{\mathbf{x}\in\boldsymbol{\theta}_j} \frac{\mathsf{d}\sigma_i \mathsf{d}\theta_j}{4\pi|\mathbf{x}-\mathbf{y}|} \\
&= \frac{|\hat{\mathbf{s}}_i, \boldsymbol{\Delta}_{j,i}, \hat{\mathbf{t}}_j|}{4\pi|\hat{\mathbf{t}}_j \times \hat{\mathbf{s}}_i|^2} \left(\arctan\frac{N_{i,j++}}{D_{i,j++}} - \arctan\frac{N_{i,j}}{D_{i,j}} - \arctan\frac{N_{i++,j++}}{D_{i++,j++}} + \arctan\frac{N_{i++,j}}{D_{i++,j}} \right) \\
&\quad + \frac{\langle \boldsymbol{\Delta}_{j++,i} \times \hat{\mathbf{s}}_i, \hat{\mathbf{t}}_j \times \hat{\mathbf{s}}_i \rangle}{4\pi|\hat{\mathbf{t}}_j \times \hat{\mathbf{s}}_i|^2} \log\frac{\Delta_{j++,i} + \Delta_{j++,i++} + \Delta_i}{\Delta_{j++,i} + \Delta_{j++,i++} - \Delta_i} \\
&\quad - \frac{\langle \boldsymbol{\Delta}_{j,i++} \times \hat{\mathbf{s}}_i, \hat{\mathbf{t}}_j \times \hat{\mathbf{s}}_i \rangle}{4\pi|\hat{\mathbf{t}}_j \times \hat{\mathbf{s}}_i|^2} \log\frac{\Delta_{j,i} + \Delta_{j,i++} + \Delta_i}{\Delta_{j,i} + \Delta_{j,i++} - \Delta_i} \\
&\quad - \frac{\langle \boldsymbol{\Delta}_{j,i++} \times \hat{\mathbf{t}}_j, \hat{\mathbf{s}}_i \times \hat{\mathbf{t}}_j \rangle}{4\pi|\hat{\mathbf{t}}_j \times \hat{\mathbf{s}}_i|^2} \log\frac{\Delta_{j,i++} + \Delta_{j++,i++} + \Delta_j}{\Delta_{j,i++} + \Delta_{j++,i++} - \Delta_j} \\
&\quad + \frac{\langle \boldsymbol{\Delta}_{j++,i} \times \hat{\mathbf{t}}_j, \hat{\mathbf{s}}_i \times \hat{\mathbf{t}}_j \rangle}{4\pi|\hat{\mathbf{t}}_j \times \hat{\mathbf{s}}_i|^2} \log\frac{\Delta_{j,i} + \Delta_{j++,i} + \Delta_j}{\Delta_{j,i} + \Delta_{j++,i} - \Delta_j}
\end{aligned} \tag{4.10}
$$

Equation (4.10) provides the solution for a projection of one edge $\boldsymbol{\sigma}_i$ of the polyhedral patch S onto an edge $\boldsymbol{\theta}_j$ of polyhedral patch T. If M and N are the number of edges/vertices of each patch, this results in $2MN$ evaluations of the `log()` function (each end vertex of an edge is the start vertex of the following edge, and therefore the `log()` only needs to be evaluated once) and MN evaluations of `atan2` (after applying all possible summation identities).

We can also notice that Equation (4.10) is rather similar to (3.1): in both cases there is a weighted sum over the 1D integrals (Lemma 2.1) followed by a sum of angles with one common weight, the normal distance of $\mathbf{x}$ to the plane of S in case of $P(\mathbf{x}, S)$ and the distance in direction $\hat{\mathbf{t}}_j \times \hat{\mathbf{s}}_i$ between the lines $\boldsymbol{\sigma}_i$ and $\boldsymbol{\theta}_j$ for $Q(\boldsymbol{\sigma}_i, \boldsymbol{\theta}_j)$ (i.e. the distance between the two planes of $\boldsymbol{\sigma}_i$ and $\boldsymbol{\theta}_j$). There is no obvious geometric interpretation for the angles, unfortunately. It remains to be seen if there are possible simplifications for the arguments, or if there is even a more general interpretation to the sum of all angles as with the solid angle interpretation of $P(\mathbf{x}, S)$. The log terms, however, are up to the weights identical in $Q(\boldsymbol{\sigma}_i, \boldsymbol{\theta}_j)$ and $P(\mathbf{x}, S)$ taking $\mathbf{x}$ as a vertex of $\boldsymbol{\sigma}_i$ or $\boldsymbol{\theta}_j$, and therefore they only have to be calculated once.

The factor in front of the log terms $\frac{\langle \boldsymbol{\Delta}_{j++,i} \times \hat{\mathbf{s}}_i, \hat{\mathbf{t}}_j \times \hat{\mathbf{s}}_i \rangle}{|\hat{\mathbf{t}}_j \times \hat{\mathbf{s}}_i|^2} = |\mathbf{o} - \mathbf{s}_i|$ can be interpreted as the distance from the four end points defining each line to the nearest point $\mathbf{o}$ to the other line, which is also the chosen origin for decomposing the homogeneous integrant in [8]. For general skewed lines, it can be obtained by minimising $|\mathbf{t}_j + t\boldsymbol{\Delta}_j - \mathbf{s}_i - s\boldsymbol{\Delta}_i|$. For co-planar lines, it becomes the distance to the crossing point between the lines. For the asymptotic case of parallel lines, the denominator $|\hat{\mathbf{t}}_j \times \hat{\mathbf{s}}_i|^2$ becomes zero and the factors singular. Yet, the solution of the parallel case is derived in Section 4.3.

4.2. Non-parallel lines with a common point

Let $\mathbf{s}_i = \mathbf{t}_j$ be the common point of $\boldsymbol{\sigma}_i$ and $\boldsymbol{\theta}_j$. The factor $|\hat{\mathbf{s}}_i, \boldsymbol{\Delta}_{j,i}, \hat{\mathbf{t}}_j| = 0$ then, as the two lines are essentially co-planar and $c = 0$ in Equation (4.4). As $\mathbf{s}_i \in \boldsymbol{\theta}_j$ and $\mathbf{t}_j \in \boldsymbol{\sigma}_i$, two of the log terms in Equation (4.10) are singular. Nevertheless, also the factors $\langle \boldsymbol{\Delta}_{j,i} \times \hat{\mathbf{s}}_i, \hat{\mathbf{t}}_j \times \hat{\mathbf{s}}_i \rangle$ are zero due to $\boldsymbol{\Delta}_{i,j} = \mathbf{s}_i - \mathbf{t}_j = \mathbf{0}$, as the origin $\mathbf{o}$ of the decomposition is identical to the common point $\mathbf{o} = \mathbf{s}_i = \mathbf{t}_j$. What remains are the two log terms projecting $\mathbf{s}_{i++}$ onto $\boldsymbol{\theta}_j$ and $\mathbf{t}_{j++}$ onto $\boldsymbol{\sigma}_i$. Equation (4.10) therefore already contains this case. The special case of two crossing lines can — although not typical for BEM — also be computed by (4.10), but the lines must be split beforehand at the crossing point.

4.3. **Parallel lines**

In the case of parallel lines, we must go back to the expression (4.3). It can be simplified considerably by noticing that the distance $|(\mathbf{x}-\mathbf{s}_i)\times\hat{\mathbf{s}}_i|$, which in this case is identical to the constant c in the previous sections, is constant for all $\mathbf{x}\in\boldsymbol{\theta}_j$. To simplify the explanations, we will assume $\langle\hat{\mathbf{s}}_i,\hat{\mathbf{t}}_j\rangle=1$ since the case $\langle\hat{\mathbf{s}}_i,\hat{\mathbf{t}}_j\rangle=-1$ (anti-parallel case) simply changes the sign of the integral. Using Lemma 4.3, it follows that

$$\begin{aligned} Q_i &= \int_{\mathbf{x}\in\boldsymbol{\theta}_j} \operatorname{arsinh}\frac{\langle\mathbf{x}-\mathbf{s}_i,\hat{\mathbf{s}}_i\rangle}{|(\mathbf{x}-\mathbf{s}_i)\times\hat{\mathbf{s}}_i|}\mathsf{d}\theta_j = \Delta_j\int_0^1 \operatorname{arsinh}\frac{\langle\boldsymbol{\Delta}_{j,i},\hat{\mathbf{s}}_i\rangle + t\langle\boldsymbol{\Delta}_j,\hat{\mathbf{s}}_i\rangle}{|\boldsymbol{\Delta}_{j,i}\times\hat{\mathbf{s}}_i|}\mathsf{d}t \\ &= \Delta_j\int_0^1 \operatorname{arsinh}(\tilde{a}_i+t\tilde{b}_i)\mathsf{d}t = \Delta_j\left[\frac{(\tilde{a}_i+\tilde{b}_i t)\operatorname{arsinh}(\tilde{a}_i+\tilde{b}_i t)-\sqrt{(\tilde{a}_i+\tilde{b}_i t)^2+1}}{\tilde{b}_i}\right]_{t=0}^{t=1} \end{aligned}$$

with the substitutions

$$\tilde{a}_i = \frac{\langle\boldsymbol{\Delta}_{j,i},\hat{\mathbf{s}}_i\rangle}{|\boldsymbol{\Delta}_{j,i}\times\hat{\mathbf{s}}_i|} \qquad \tilde{b}_i = \frac{\langle\boldsymbol{\Delta}_j,\hat{\mathbf{s}}_i\rangle}{|\boldsymbol{\Delta}_{j,i}\times\hat{\mathbf{s}}_i|} = \frac{\Delta_j}{|\boldsymbol{\Delta}_{j,i}\times\hat{\mathbf{s}}_i|}$$

Re-substituting gives the solution

$$\begin{aligned} Q_i = \Delta_j\Bigg(&\frac{\langle\boldsymbol{\Delta}_{j++,i},\hat{\mathbf{s}}_i\rangle}{\Delta_j}\operatorname{arsinh}\frac{\langle\boldsymbol{\Delta}_{j++,i},\hat{\mathbf{s}}_i\rangle}{|\boldsymbol{\Delta}_{j,i}\times\hat{\mathbf{s}}_i|} - \frac{\langle\boldsymbol{\Delta}_{j,i},\hat{\mathbf{s}}_i\rangle}{\Delta_j}\operatorname{arsinh}\frac{\langle\boldsymbol{\Delta}_{j,i},\hat{\mathbf{s}}_i\rangle}{|\boldsymbol{\Delta}_{j,i}\times\hat{\mathbf{s}}_i|} \\ &-\frac{\sqrt{\langle\boldsymbol{\Delta}_{j++,i},\hat{\mathbf{s}}_i\rangle^2+|\boldsymbol{\Delta}_{j,i}\times\hat{\mathbf{s}}_i|^2}}{\Delta_j} + \frac{\sqrt{\langle\boldsymbol{\Delta}_{j,i},\hat{\mathbf{s}}_i\rangle^2+|\boldsymbol{\Delta}_{j,i}\times\hat{\mathbf{s}}_i|^2}}{\Delta_j}\Bigg) \end{aligned}$$

Noting $|\boldsymbol{\Delta}_{j,i}\times\hat{\mathbf{s}}_i| = |\boldsymbol{\Delta}_{j++,i}\times\hat{\mathbf{s}}_i| = |\boldsymbol{\Delta}_{j,i++}\times\hat{\mathbf{s}}_i| = |\boldsymbol{\Delta}_{j++,i++}\times\hat{\mathbf{s}}_i|$ by parallelism, $\boldsymbol{\Delta}_j = \mathbf{t}_{j++}-\mathbf{t}_j = \Delta_j\hat{\mathbf{t}}_j$ and $\sqrt{\langle\boldsymbol{\Delta}_{j,i},\hat{\mathbf{s}}_i\rangle^2+|\boldsymbol{\Delta}_{j,i}\times\hat{\mathbf{s}}_i|^2} = \Delta_{j,i}$, as well as using (4.3) gives

$$\begin{aligned} Q(\boldsymbol{\sigma}_i\parallel\boldsymbol{\theta}_j) &= \frac{1}{4\pi}(Q_i-Q_{i++}) \\ &= \frac{\langle\boldsymbol{\Delta}_{j++,i},\hat{\mathbf{s}}_i\rangle}{4\pi}\operatorname{arsinh}\frac{\langle\boldsymbol{\Delta}_{j++,i},\hat{\mathbf{s}}_i\rangle}{|\boldsymbol{\Delta}_{j,i}\times\hat{\mathbf{s}}_i|} - \frac{\langle\boldsymbol{\Delta}_{j,i},\hat{\mathbf{s}}_i\rangle}{4\pi}\operatorname{arsinh}\frac{\langle\boldsymbol{\Delta}_{j,i},\hat{\mathbf{s}}_i\rangle}{|\boldsymbol{\Delta}_{j,i}\times\hat{\mathbf{s}}_i|} \\ &\quad - \frac{\langle\boldsymbol{\Delta}_{j++,i++},\hat{\mathbf{s}}_i\rangle}{4\pi}\operatorname{arsinh}\frac{\langle\boldsymbol{\Delta}_{j++,i++},\hat{\mathbf{s}}_i\rangle}{|\boldsymbol{\Delta}_{j,i}\times\hat{\mathbf{s}}_i|} + \frac{\langle\boldsymbol{\Delta}_{j,i++},\hat{\mathbf{s}}_i\rangle}{4\pi}\operatorname{arsinh}\frac{\langle\boldsymbol{\Delta}_{j,i++},\hat{\mathbf{s}}_i\rangle}{|\boldsymbol{\Delta}_{j,i}\times\hat{\mathbf{s}}_i|} \\ &\quad + \frac{1}{4\pi}(-\Delta_{j++,i}+\Delta_{j,i}+\Delta_{j++,i++}-\Delta_{j,i++}) \end{aligned} \tag{4.11}$$

The equation above is equivalent to the solution given by [11]. Equation (4.11) shows that also the asymptotic case of parallel lines in Equation (4.10) has a non-singular solution. It remains to be seen if an equivalent solution to (4.10) can be found that includes the parallel case and does not require a separate treatment.

Remark 4.4. Let us remark that the particular case of identical lines $\boldsymbol{\theta}_j=\boldsymbol{\sigma}_i$ is known to be weakly singular but does not raises difficulty. Indeed, coming back to formula (2.6) we see that the self-influence case is multiplied by $d(\mathbf{s}_i,\boldsymbol{\theta}_j)=0$.

5. The hypersingular kernel on polyhedral domains

For solving the hypersingular kernel, it is helpful to first redefine it with respect to some solenoidal vector potential $\mathbf{A}$ fulfilling the vector Poisson equation

$$\Delta\mathbf{A} = -\nabla\times(\nabla\times\mathbf{A}) = \omega \;\rightarrow \mathbf{A}(\mathbf{y}) = \int_{\mathbf{x}\in\partial\Omega} \frac{\omega}{4\pi|\mathbf{x}-\mathbf{y}|}\mathsf{d}S \tag{5.1}$$

Theorem 5.1. *The hypersingular kernel can be written as a double line integral*

$$W = \sum_i\sum_j \oint_{\mathbf{y}\in\partial\boldsymbol{\sigma}_i}\oint_{\mathbf{x}\in\boldsymbol{\theta}_j} \langle \mathsf{d}\boldsymbol{\sigma}_i, \mathsf{d}\boldsymbol{\theta}_j\rangle G(\mathbf{x},\mathbf{y}) \tag{5.2}$$

Proof. Using (2.3), replacing $\partial/\partial\mathbf{n} = \mathbf{n}\cdot\nabla$ gives

$$\begin{aligned} W &= \int_{\mathbf{y}\in S}\int_{\mathbf{x}\in T} \frac{\partial^2 G(\mathbf{x},\mathbf{y})}{\partial\mathbf{n}_S\partial\mathbf{n}_T}\mathsf{d}T\mathsf{d}S \\ &= \int_{\mathbf{y}\in S}\mathbf{n}_S\cdot\nabla_{\mathbf{y}}\left[\int_{\mathbf{x}\in T}\mathbf{n}_T\cdot\nabla_{\mathbf{x}}G(\mathbf{x},\mathbf{y})\mathsf{d}T\right]\mathsf{d}S \end{aligned}$$

The outer integral, the Neumann boundary conditions integrated over the surface patch S_i, is replaced by

$$\int_{\mathbf{y}\in S}\mathbf{n}_S\cdot\nabla_{\mathbf{y}}\Phi(\mathbf{y})\mathsf{d}S = \int_{\mathbf{y}\in S}\mathbf{n}_S\cdot\nabla_{\mathbf{y}}\times\mathbf{A}(\mathbf{y})\mathsf{d}S = \oint_{\mathbf{y}\in\partial S}\mathbf{A}(\mathbf{y})\cdot\mathsf{d}\boldsymbol{\sigma}_i\ ,$$

the only difference is the fact that the vector field in the integrant is now obtained by the curl of a vector field $\mathbf{A}(\mathbf{y})$ (the new inner integral) instead of the gradient of a potential $\Phi(\mathbf{y})$, the previous inner integral as written above. This is possible for all solenoidal vector fields. Applying Stokes' theorem yields the outer line integral over the boundary ∂S of S.

For the treatment of the inner integral, a change in variables is necessary. Equation (2.3) is derived for a uniform distribution of the double layer potential μ (also dipole or double distribution). The surface vorticity distribution is related to the double layer potential μ by the gradient rotated around the normal $\omega = \mathbf{n}\times\nabla\mu = \nabla\times(\mu\mathbf{n})$. In the usual definition of the hypersingular kernel, the double layer potential μ is a piecewise constant distribution of unit strength, therefore the equivalent surface vorticity distribution is only defined at the boundary ∂T as

$$\omega(\mathbf{x}) = \mathbf{n}\times\nabla\mu(\mathbf{x}) = \mathbf{n}\times\mathbf{b}(\mathbf{x})\delta(\mathbf{x}-\mathbf{x}') \quad \forall\mathbf{x}'\in\partial T$$

with the outward-pointing binormal $\mathbf{b}$ to the boundary ∂S_j. The cross product between the normal and the binormal is the unit tangent vector $\mathbf{t} = \mathbf{n}\times\mathbf{b}$. Using all this with the definition of the vector potential (5.1) yields

$$\begin{aligned} \mathbf{A}(\mathbf{y}) &= \int_{\mathbf{x}\in T}\omega G(\mathbf{x},\mathbf{y})\mathsf{d}T \\ &= \int_{\mathbf{x}\in T}\mathbf{n}\times\nabla\mu G(\mathbf{x},\mathbf{y})\mathsf{d}T \\ &= \int_{\mathbf{x}\in T}\mathbf{t}\delta(\mathbf{x}-\mathbf{x}')G(\mathbf{x},\mathbf{y})\mathsf{d}T \\ &= \oint_{\mathbf{x}'\in\partial T}G(\mathbf{x}',\mathbf{y})\mathsf{d}\boldsymbol{\theta}_j \end{aligned}$$

Dropping the superscript and putting the inner into the outer integral gives (5.2). ■

A more general proof of the reduction of the hypersingular kernel of a dipole distribution to a weakly singular kernel of the vorticity distribution is given in [12]. The important point for this work is that this reduction step simultaneously reduces the dimension of the integrals from four to two, as far as flat surface patches with piecewise constant dipole distributions are concerned.

The change in variables above is analogous to what can be found in the classical literature on the Boundary Element Method. The equivalence of a piecewise constant dipole panel/patch with a line vortex of constant strength at the boundary of the patch was already proven by [7].

6. Conclusion

This paper summarises the results obtained in an ongoing project with the aim to find optimized and general closed-form solutions of the Galerkin BEM integrals on polyhedral domains. The solutions found by Lenoir&Salles for the $P(\mathbf{x}, S)$ and $Q(\partial S, \partial T)$ integrals can be improved or respectively generalized. Solving the integral $P(\mathbf{x}, S)$ is already required in the Collocation Point method, therefore an extensive list of literature is available and all parts have thoroughly been optimized. A solution for general skewed lines can also be derived for the integral $Q(\partial S, \partial T)$, although a special treatment of parallel lines is still required.

Moreover, some result suggests that different decompositions of the integrals are possible, which is promising for other integrals in the decomposition. Singularities in the solutions are another point for further optimization work, as these require costly treatments in parallelized implementations. Eventually, the analytical approach to the Galerkin method is very promising but remains an interesting problem.

Acknowledgements

C. Gout and Z. Lambert thank Albert Cohen and the organizing committee of the Ninth International conference Curves and Surfaces, they also thank Avenia pole, Labex AMIES and MSO net for their support to organise this mini symposium. I. Ciotir, C. Gout, Z. Lambert and A. Tonnoir thank M2NUM project (M2NUM is co-financed by the European Union with the European regional development fund (ERDF, HN0002137) and by Région Normandie), they also thank M2SiNum project (M2SiNum is co-financed by the European Union with the European regional development fund (ERDF, 18P03390/18E01750/18P02733) and by Région Normandie). N. Warncke thanks the INWIT and WAKE OP projects co-financed by Région Normandie. I Ciotir thanks the ANR QUTE-HPC project (ANR-18-CE46-0013).

Appendix A. Proof of Lemma 2.1

Lemma 2.1. *The solutions of the 1D integral over the weakly singular kernel are*

$$\int_{\mathbf{y}\in\boldsymbol{\sigma}_i} \frac{1}{4\pi|\mathbf{x}-\mathbf{y}|}\mathsf{d}\sigma_i = -\frac{1}{4\pi}\log\frac{\langle\mathbf{x}-\mathbf{s}_{i++},\hat{\mathbf{s}}_i\rangle + |\mathbf{x}-\mathbf{s}_{i++}|}{\langle\mathbf{x}-\mathbf{s}_i,\hat{\mathbf{s}}_i\rangle + |\mathbf{x}-\mathbf{s}_i|} \tag{2.7a}$$

$$= \frac{1}{4\pi}\log\frac{|\mathbf{x}-\mathbf{s}_{i++}| - \langle\mathbf{x}-\mathbf{s}_{i++},\hat{\mathbf{s}}_i\rangle}{|\mathbf{x}-\mathbf{s}_i| - \langle\mathbf{x}-\mathbf{s}_i,\hat{\mathbf{s}}_i\rangle} \tag{2.7b}$$

$$= -\frac{1}{4\pi}\log\frac{|\mathbf{x}-\mathbf{s}_i| + |\mathbf{x}-\mathbf{s}_{i++}| + |\mathbf{s}_{i++}-\mathbf{s}_i|}{|\mathbf{x}-\mathbf{s}_i| + |\mathbf{x}-\mathbf{s}_{i++}| - |\mathbf{s}_{i++}-\mathbf{s}_i|} \tag{2.7c}$$

$$= -\frac{1}{2\pi}\operatorname{arcoth}\frac{|\mathbf{x}-\mathbf{s}_i| + |\mathbf{x}-\mathbf{s}_{i++}|}{|\mathbf{s}_{i++}-\mathbf{s}_i|} \tag{2.7d}$$

$$= -\frac{1}{4\pi}\left(\operatorname{arsinh}\frac{\langle\mathbf{x}-\mathbf{s}_{i++},\hat{\mathbf{s}}_i\rangle}{|(\mathbf{x}-\mathbf{s}_{i++})\times\hat{\mathbf{s}}_i|} - \operatorname{arsinh}\frac{\langle\mathbf{x}-\mathbf{s}_i,\hat{\mathbf{s}}_i\rangle}{|(\mathbf{x}-\mathbf{s}_i)\times\hat{\mathbf{s}}_i|}\right) \tag{2.7e}$$

Proof. First we have

$$\frac{1}{4\pi}\int_{\mathbf{y}\in\boldsymbol{\sigma}_i}\frac{1}{|\mathbf{x}-\mathbf{y}|}\mathsf{d}\sigma_i = \frac{|\mathbf{s}_{i++}-\mathbf{s}_i|}{4\pi}\int_0^1 \frac{\mathsf{d}s}{\sqrt{(\mathbf{x}-(\mathbf{s}_i+s(\mathbf{s}_{i++}-\mathbf{s}_i)))^2}}$$

$$= \frac{1}{4\pi}\int_0^1 \frac{\mathrm{d}s}{\sqrt{a^2+(s-b)^2}}$$

$$= \frac{1}{4\pi}\left[-\log\left(\sqrt{a^2+(s-b)^2}+(b-s)\right)\right]_0^1$$

$$= \frac{-1}{4\pi}\log\frac{\sqrt{a^2+(b-1)^2}+b-1}{\sqrt{a^2+b^2}+b}$$

with

$$a^2 = \frac{(\mathbf{x}-\mathbf{s}_i)^2}{(\mathbf{s}_{i++}-\mathbf{s}_i)^2} - b^2 = \frac{((\mathbf{x}-\mathbf{s}_i)\times\hat{\mathbf{s}}_i)^2}{(\mathbf{s}_{i++}-\mathbf{s}_i)^2}$$

and

$$b = \frac{\langle\mathbf{x}-\mathbf{s}_i,\mathbf{s}_{i++}-\mathbf{s}_i\rangle}{(\mathbf{s}_{i++}-\mathbf{s}_i)^2} \quad\text{and}\quad b-1 = \frac{\langle\mathbf{x}-\mathbf{s}_{i++},\mathbf{s}_{i++}-\mathbf{s}_i\rangle}{(\mathbf{s}_{i++}-\mathbf{s}_i)^2}.$$

Let us remark that to get the second expression of a we have used the classical equality

$$|\mathbf{u}|^2|\mathbf{v}|^2 = \langle\mathbf{u},\mathbf{v}\rangle^2 + |\mathbf{u}\times\mathbf{v}|^2 \tag{A.2}$$

with $\mathbf{u} = \mathbf{x}-\mathbf{s}_i$ and $\mathbf{v} = \hat{\mathbf{s}}_i$ and we recall that $\hat{\mathbf{s}}_i = \frac{\mathbf{s}_{i++}-\mathbf{s}_i}{|\mathbf{s}_{i++}-\mathbf{s}_i|}$.
The above expression of the integral gives (2.7a) after reversing the substitutions to get:

$$\sqrt{a^2+b^2}+b = \frac{\langle\mathbf{x}-\mathbf{s}_i,\mathbf{s}_{i++}-\mathbf{s}_i\rangle}{(\mathbf{s}_{i++}-\mathbf{s}_i)^2} + \frac{|\mathbf{x}-\mathbf{s}_i|}{|\mathbf{s}_{i++}-\mathbf{s}_i|} = \frac{\langle\mathbf{x}-\mathbf{s}_i,\hat{\mathbf{s}}_i\rangle + |\mathbf{x}-\mathbf{s}_i|}{|\mathbf{s}_{i++}-\mathbf{s}_i|}$$

and

$$\sqrt{a^2+(b-1)^2}+(b-1)=\frac{\langle \mathbf{x}-\mathbf{s}_{i++},\mathbf{s}_{i++}-\mathbf{s}_i\rangle}{(\mathbf{s}_{i++}-\mathbf{s}_i)^2}+\sqrt{\frac{(\mathbf{x}-\mathbf{s}_i\times\hat{\mathbf{s}}_i)^2}{(\mathbf{s}_{i++}-\mathbf{s}_i)^2}+\frac{\langle \mathbf{x}-\mathbf{s}_{i++},\mathbf{s}_{i++}-\mathbf{s}_i\rangle^2}{(\mathbf{s}_{i++}-\mathbf{s}_i)^4}}$$

$$=\frac{\langle \mathbf{x}-\mathbf{s}_{i++},\hat{\mathbf{s}}_i\rangle}{|\mathbf{s}_{i++}-\mathbf{s}_i|}+\sqrt{\frac{(\mathbf{x}-\mathbf{s}_i\times\hat{\mathbf{s}}_i)^2+\langle \mathbf{x}-\mathbf{s}_{i++},\hat{\mathbf{s}}_i\rangle^2}{(\mathbf{s}_{i++}-\mathbf{s}_i)^2}}$$

$$=\frac{\langle \mathbf{x}-\mathbf{s}_{i++},\hat{\mathbf{s}}_i\rangle+|\mathbf{x}-\mathbf{s}_{i++}|}{|\mathbf{s}_{i++}-\mathbf{s}_i|}$$

The last equality is obtained thanks to (A.2) and using the fact that $\mathbf{x}-\mathbf{s}_i\times\hat{\mathbf{s}}_i=\mathbf{x}-\mathbf{s}_{i++}\times\hat{\mathbf{s}}_i$. In all cases, $\sqrt{a^2+b^2}\geq|b|\quad\forall b\in\mathbb{R}$, such that both the numerator and the denominator of the log are well-defined for $|a|>0$. For $a=0$, $\mathbf{x}$ lies on the extension of the edge $\boldsymbol{\sigma}_i$ and the solution has a logarithmic singularity for $b\leq 1$. Equation (2.7b) can easily be deduced noticing that another expression of the primitive of $\sqrt{a^2+(s-b)^2}^{-1}$ is given by

$$\int_0^1\frac{\mathsf{d}s}{\sqrt{a^2+(s-b)^2}}=\left[\log\left(\sqrt{a^2+(s-b)^2}+(s-b)\right)\right]_0^1$$

where as previously const. is a constant term. This formula can also be obtained for $a=0$ by subtracting the singularity [4]. This solution has a logarithmic singularity for $a=0$ and $b\geq 0$.
The equivalence of (2.7a) with (2.7c) was shown by [6]: noting that $\langle\mathbf{x}-\mathbf{s}_i,\hat{\mathbf{s}}_i\rangle+|\mathbf{x}-\mathbf{s}_i|=|\mathbf{x}-\mathbf{s}_i|(1-\cos\beta_i)$ with $\cos\beta_i=\frac{\langle\mathbf{x}-\mathbf{s}_i,\hat{\mathbf{s}}_i\rangle}{|\mathbf{x}-\mathbf{s}_i|}$ and applying the law of cosines $\cos\beta_i=\frac{|\mathbf{x}-\mathbf{s}_i|^2-|\mathbf{x}-\mathbf{s}_{i++}|^2+|\mathbf{s}_{i++}-\mathbf{s}_i|^2}{2|\mathbf{x}-\mathbf{s}_i||\mathbf{s}_{i++}-\mathbf{s}_i|}$ and $\cos\beta_{i++}=\frac{|\mathbf{x}-\mathbf{s}_i|^2-|\mathbf{x}-\mathbf{s}_{i++}|^2-|\mathbf{s}_{i++}-\mathbf{s}_i|^2}{2|\mathbf{x}-\mathbf{s}_{i++}||\mathbf{s}_{i++}-\mathbf{s}_i|}$ to both the numerator and the denominator yields

$$\frac{\langle\mathbf{x}-\mathbf{s}_{i++},\hat{\mathbf{s}}_i\rangle+|\mathbf{x}-\mathbf{s}_{i++}|}{\langle\mathbf{x}-\mathbf{s}_i,\hat{\mathbf{s}}_i\rangle+|\mathbf{x}-\mathbf{s}_i|}=\frac{2|\mathbf{x}-\mathbf{s}_{i++}||\mathbf{s}_{i++}-\mathbf{s}_i|-|\mathbf{x}-\mathbf{s}_i|^2+|\mathbf{x}-\mathbf{s}_{i++}|^2+|\mathbf{s}_{i++}-\mathbf{s}_i|^2}{2|\mathbf{x}-\mathbf{s}_i||\mathbf{s}_{i++}-\mathbf{s}_i|-|\mathbf{x}-\mathbf{s}_i|^2+|\mathbf{x}-\mathbf{s}_{i++}|^2-|\mathbf{s}_{i++}-\mathbf{s}_i|^2}$$

$$=\frac{(|\mathbf{x}-\mathbf{s}_{i++}|-|\mathbf{x}-\mathbf{s}_i|+|\mathbf{s}_{i++}-\mathbf{s}_i|)(|\mathbf{x}-\mathbf{s}_{i++}|+|\mathbf{x}-\mathbf{s}_i|+|\mathbf{s}_{i++}-\mathbf{s}_i|)}{(|\mathbf{x}-\mathbf{s}_{i++}|-|\mathbf{x}-\mathbf{s}_i|+|\mathbf{s}_{i++}-\mathbf{s}_i|)(|\mathbf{x}-\mathbf{s}_{i++}|+|\mathbf{x}-\mathbf{s}_i|-|\mathbf{s}_{i++}-\mathbf{s}_i|)}$$

$$=\frac{|\mathbf{x}-\mathbf{s}_{i++}|+|\mathbf{x}-\mathbf{s}_i|+|\mathbf{s}_{i++}-\mathbf{s}_i|}{|\mathbf{x}-\mathbf{s}_{i++}|+|\mathbf{x}-\mathbf{s}_i|-|\mathbf{s}_{i++}-\mathbf{s}_i|}$$

Solution (2.7c) has a logarithmic singularity only for $a=0$ and $b\in[0,1]$, or for $\mathbf{x}\in\boldsymbol{\sigma}_i$, and it is also numerically the most robust solution[6]. Equation (2.7d) is obtained from (2.7c) by using the definition of the inverse hyperbolic cotangens via the logarithm $\operatorname{arcoth}(x)=\frac{1}{2}\log\frac{x+1}{x-1}$. Also this solution has a singularity for $\mathbf{x}\in\boldsymbol{\sigma}_i$, there the argument of the function becomes 1. Finally, (2.7e) is obtained from the definition of the inverse hyperbolic sinus $\operatorname{arsinh}(x)=\log(x+\sqrt{x^2+1})$ and $|\mathbf{x}-\mathbf{s}_i|^2=\langle\mathbf{x}-\mathbf{s}_i,\hat{\mathbf{s}}_i\rangle^2+|(\mathbf{x}-\mathbf{s}_i)\times\hat{\mathbf{s}}_i|^2$. This solution is singular for all points in the extension of $\boldsymbol{\sigma}_i$. ∎

Appendix B. Proof of Lemma 4.2

Lemma 4.2.

$$\int\operatorname{arsinh}\frac{a+bz}{\sqrt{c^2+z^2}}\mathsf{d}z=z\operatorname{arsinh}\frac{a+bz}{\sqrt{z^2+c^2}}-c\arctan\frac{az-bc^2}{c\sqrt{(a+bz)^2+z^2+c^2}}$$
$$+\frac{a}{\sqrt{b^2+1}}\log(\sqrt{b^2+1}\sqrt{(a+bz)^2+z^2+c^2}+b(a+bz)+z)+\text{const.}\qquad(4.4)$$

Proof. Taking the derivatives of each term gives:

$$\frac{\mathsf{d}}{\mathsf{d}z}\left(z\operatorname{arsinh}\frac{a+bz}{\sqrt{z^2+c^2}}\right) = \operatorname{arsinh}\frac{a+bz}{\sqrt{z^2+c^2}} + z\left(\frac{\frac{b}{\sqrt{z^2+c^2}} - \frac{z(a+bz)}{\sqrt{z^2+c^2}^3}}{\sqrt{\frac{(a+bz)^2}{z^2+c^2}+1}}\right)$$

$$= \operatorname{arsinh}\frac{a+bz}{\sqrt{z^2+c^2}} + \frac{z(bc^2-za)}{(z^2+c^2)\sqrt{(a+bz)^2+z^2+c^2}}$$

$$\frac{\mathsf{d}}{\mathsf{d}z}\left(c\arctan\frac{az-bc^2}{c\sqrt{(a+bz)^2+z^2+c^2}}\right) = c\frac{\frac{a}{c\sqrt{(a+bz)^2+z^2+c^2}} - \frac{(az-bc^2)(b(a+bz)+z)}{c\sqrt{(a+bz)^2+z^2+c^2}^3}}{1+\frac{(az-bc^2)^2}{c^2((a+bz)^2+z^2+c^2)}}$$

$$= \frac{c^2(a(a+bz)^2+az^2+ac^2-(az-bc^2)(ba+b^2z+z))}{(c^2a^2+2abzc^2+c^2b^2z^2+c^2z^2+c^4+a^2z^2-2azbc^2+b^2c^4)\sqrt{(a+bz)^2+z^2+c^2}}$$

$$= \frac{c^2(a(a+bz)^2-azb(a+bz)+ac^2(b^2+1)+zbc^2(b^2+1))}{(z^2+c^2)(a^2+c^2+c^2b^2)\sqrt{(a+bz)^2+z^2+c^2}}$$

$$= \frac{c^2(a+bz)}{(z^2+c^2)\sqrt{(a+bz)^2+z^2+c^2}}$$

$$\frac{\mathsf{d}}{\mathsf{d}z}\left(\frac{a}{\sqrt{b^2+1}}\log(\sqrt{b^2+1}\sqrt{(a+bz)^2+z^2+c^2}+b(a+bz)+z)\right)$$

$$= \frac{a\left(\sqrt{b^2+1}\frac{(a+bz)b+z}{\sqrt{(a+bz)^2+z^2+c^2}}+b^2+1\right)}{\sqrt{b^2+1}(\sqrt{b^2+1}\sqrt{(a+bz)^2+z^2+c^2}+b(a+bz)+z)}$$

$$= \frac{a\left((a+bz)b+z+\sqrt{b^2+1}\sqrt{(a+bz)^2+z^2+c^2}\right)}{\sqrt{(a+bz)^2+z^2+c^2}(\sqrt{b^2+1}\sqrt{(a+bz)^2+z^2+c^2}+b(a+bz)+z)}$$

$$= \frac{a}{\sqrt{(a+bz)^2+z^2+c^2}} = \frac{a(z^2+c^2)}{(z^2+c^2)\sqrt{(a+bz)^2+z^2+c^2}}$$

Summing all terms up leaves only the arsinh term:

$$\frac{\mathsf{d}}{\mathsf{d}z}\Bigg(z\operatorname{arsinh}\frac{a+bz}{\sqrt{z^2+c^2}} - c\arctan\frac{az-bc^2}{c\sqrt{(a+bz)^2+z^2+c^2}}$$

$$+\frac{a}{\sqrt{b^2+1}}\log(\sqrt{b^2+1}\sqrt{(a+bz)^2+z^2+c^2}+b(a+bz)+z)\Bigg)$$

$$= \operatorname{arsinh}\frac{a+bz}{\sqrt{z^2+c^2}} + \frac{z(bc^2-za)-c^2(a+bz)+a(z^2+c^2)}{(z^2+c^2)\sqrt{(a+bz)^2+z^2+c^2}} = \operatorname{arsinh}\frac{a+bz}{\sqrt{z^2+c^2}}$$

■

Appendix C. Proof of Lemma 4.3

Lemma 4.3.

$$\int \operatorname{arsinh}(a+bz)\mathsf{d}z = \frac{(a+bz)\operatorname{arsinh}(a+bz)-\sqrt{(a+bz)^2+1}}{b} + \text{const.} \tag{4.5}$$

Proof.

$$\frac{\mathsf{d}}{\mathsf{d}z}\left(\int \operatorname{arsinh}(a+bz)\mathsf{d}z\right) = \operatorname{arsinh}(a+bz) + \left(\frac{a}{b}+z\right)\left(\frac{b}{\sqrt{(a+bz)^2+1}}\right) - \frac{b(a+bz)}{b\sqrt{(a+bz)^2+1}}$$
$$= \operatorname{arsinh}(a+bz)$$

■

Appendix D. Siemens-Gamesa renewable energy

The new Siemens Gamesa Renewable Energy Group (SGRE)[1] was born in April 2017, with the merger of Gamesa Corporación Tecnológica and Siemens Wind Power.

Gamesa's history is marked by a spirit of innovation and successful expansion into new markets. What started as a small machining workshop in northern Spain quickly grew into a global Company focused on industrial facility management, the automotive industry, and new technology development.

In 1995, Gamesa expanded into wind power, installing the first wind turbine in the hills of El Perdón, in Spain, and just four years later the Company had grown into the leading manufacturer of wind turbines in the country. International expansion quickly followed as the Company opened production centers in the U.S., China, India and Brazil. The history of Siemens Wind Power is equally impressive.

The Company has been directly involved in the wind power industry since 2004, when it acquired the Danish wind turbine manufacturer Bonus Energy. With the acquisition of Bonus, Siemens gained a wealth of technology and proven experience stretching back to 1980. This history includes providing turbines for the world's first offshore wind farm located in Vindeby off the coast of Denmark, in 1991. The Company grew into the global market leader for offshore wind turbines, earning a reputation for technological leadership, strong customer service, and for offering fully integrated end-to-end energy solutions. Siemens Gamesa Renewable Energy brings these many qualities together under one roof: an innovative spirit, dedication to technological excellence, and a determination to provide real and lasting value to all stakeholders and customers.

Today, Siemens Gamesa Renewable Energy is a respected industry leader committed to providing innovative and effective solutions to the energy challenges of tomorrow. Siemens Gamesa Renewable Energy came into being ready to address the challenges and seize the opportunities that the wind business offers in the short, medium and long term, to create value for all stakeholders. In a changing environment with increasingly demanding wind markets, the merger's strategic rationale is even more compelling. Global scale and reach have become essential to compete profitably. Meanwhile, the combined Company's diversification and balance and its leading position in emerging and offshore markets provide resilience and above-average growth potential.

Key Facts (as of September 30, 2018):

- 89 GW: Total installed capacity.
- 23k: Employees worldwide.
- Onshore: 76.9 GW installed in 75 countries. The perfect technology partner for your wind projects.
- Offshore: 12.5 GW installed worldwide since 1991. Most experienced offshore wind company with the most reliable product portfolio in the market.
- Service: 56.7 GW maintained. Commitment beyond the supply of the wind turbine to achieve the profitability objectives of each project.

[1] `https://www.siemensgamesa.com`

References

[1] A. Abdelsalam. Higher-Order Panel Method for Wind Turbine Flow Solver. Master's thesis, École Polytechnique (France), 2015.

[2] Z. ambert, C. Gout, J. Baccou, H. Calandra, J. Caruso, and N. G. W. Warncke. Mathematical tools in energy industry. *Matapli*, 118:23–38, 2019.

[3] H. Calandra, Z. Lambert, C. Gout, A. Atle, M. Bonnasse-Gahot, J. Diaz, and S. Ettouati. Recent advances in numerical methods for solving the wave equation in the context of seismic depth imaging. *SMAI J. Comput. Math.*, 2019. to appear.

[4] J. D'Eliá, M. Storti, and S. Idelsohn. A closed form for low-order panel methods. *Advances in Engineering Software*, 31(5):347–353, 2000.

[5] C. Gout, Z. Lambert, and D. Apprato. *Data approximation : mathematical modelling and numerical simulations.* EDP Sciences, 2019.

[6] J. L. Hess and A. M. O. Smith. Calculation of non-lifting potential flow about arbitrary three-dimensional bodies. Technical report, Douglas Aircraft Co Long Beach CA, 1962.

[7] J. L. Hess and A. M. O. Smith. Calculation of potential flow about arbitrary bodies. *Progress in Aerospace Sciences*, 8:1–138, 1967.

[8] M. Lenoir and N. Salles. Evaluation of 3-D singular and nearly singular integrals in Galerkin BEM for thin layers. *SIAM J. Sci. Comput.*, 34(6):A3057–A3078, 2012.

[9] M. Lenoir and N. Salles. Exact evaluation of singular and near-singular integrals in Galerkin BEM. *Proceedings of ECCOMAS 2012*, pages 1–20, 2012.

[10] F. W. J. Olver, D. W. Lozier, R. F. Boisvert, and C. W. Clark, editors. *NIST handbook of mathematical functions hardback and CD-ROM.* Cambridge University Press, 2010.

[11] N. Salles. *Calculation of singularities in variational integral equations methods.* PhD thesis, Université Paris Sud - Paris XI (France), 2013. `https://pastel.archives-ouvertes.fr/tel-00877482`.

[12] S. A. Sauter and C. Schwab. Boundary Element Methods. In *Boundary Element Methods*, pages 183–287. Springer, 2010.

[13] A. Van Oosterom and J. Strackee. The solid angle of a plane triangle. *IEEE transactions on Biomedical Engineering*, BME-30(2):125–126, 1983.